PREDICTING OCCUPIED ZONE TEMPERATURE USING SIMPLIFIED MODELING METHODS

A Thesis
By
PHILIP WILLIAM HOWARD

Submitted to the Graduate School
at Appalachian State University
in partial fulfillment of the requirements for the degree of
MASTER OF SCIENCE

December 2019
Department of Sustainable Technology & the Built Environment

PREDICTING OCCUPIED ZONE TEMPERATURE USING SIMPLIFIED MODELING METHODS

A Thesis
by
PHILIP WILLIAM HOWARD
December 2019

APPROVED BY:

Dr. Jeff Ramsdell
Chairperson, Thesis Committee

Dr. Marie Hoepfl
Member, Thesis Committee

Dr. Andrew Windham
Member, Thesis Committee

Dr. Brian W. Raichle
Chairperson, Department of Sustainable Technology & the Built Environment

Dr. Mike McKenzie
Dean, Cratis D. Williams School of Graduate Studies

ABSTRACT

PREDICTING OCCUPIED ZONE TEMPERATURE USING SIMPLIFIED MODELING METHODS

Philip William Howard

B.S., Appalachian State University

M.S., Appalachian State University

Chairperson: Dr. Jeff Ramsdell

Due to the expected level of thermal stratification that is present in buildings which are subject to high levels of infiltration during the heating season, the well mixed modeling approach may not be the most appropriate method for modeling interior conditions and energy use in structures with low levels of insulation and poor air sealing. A simplified modeling method known as the Three-Node Displacement Ventilation RoomAir Model was developed by da Graça (2003) for predicting levels of thermal stratification present in buildings that utilize displacement ventilation systems (DV). This paper examines the level of thermal stratification in a building with no forced air that is subject to high levels of infiltration during the heating season, and the ability of the Three-Node Displacement Ventilation RoomAir Model to accurately model the thermal stratification therein. It was found that the levels of thermal stratification in the test building were such that the well mixed modeling approach is not appropriate. However, the Three-Node Displacement Ventilation RoomAir Model was also found to be inappropriate for modeling the conditions set forth in this research due to the methods for predicting temperature distribution utilized in the model. It was concluded that

another method for modeling thermal stratification in loosely constructed buildings during the heating season should be developed.

Acknowledgments

This research would not have been possible without the support of my thesis committee. I will be forever grateful for all the encouragement, understanding, and motivation that they, and many other faculty and staff at Appalachian State University, have shown me over the course of my education. My time at Appalachian State is one that I will forever cherish. Thank you.

Table of Contents

List of Tables

List of Figures

CHAPTER 1: INTRODUCTION

According to the Population Reference Bureau (2018), by 2050 the number of people on the planet will have increased from the current estimated world population of 7.6 billion people, to around 9.9 billion people, which is a 29% increase. It is estimated that 97% of this growth will occur in developing nations (Walker, 2016). This means that there is likely going to be a large increase in the need for housing in these same areas. According to a study done by Daioglou, Van Ruijven, and Van Vuuren (2012), residential energy use accounts for approximately 35% of the global total. While residential energy use in developing nations is substantially lower than residential energy use in developed nations, considering that the majority of population growth will occur in developing nations, residential energy in these nations will continue to account for a larger portion of the global residential energy use as time moves on. For this reason, it is crucial that residential development is approached in a way that is more sustainable and energy efficient than it has been in the past.

Internationally, it is a historically common approach to view housing affordability solely in terms of economic viability, with little or no regard to sustainability or life cycle costs (Mulliner, Smallbone & Maliene, 2013). As more research is being done on building performance and energy use, tools and bodies of knowledge have been developed that might aid in building higher performing, and more energy efficient buildings. One such tool is Building Energy Modeling (BEM) Software. These softwares can predict a building's occupancy comfort, energy use, and many other things, using applicable historic on-site weather data. One example of such a BEM software is EnergyPlus™.

EnergyPlus™ is a program that allows the user to perform energy analysis while simulating thermal loads, all based on user inputs that coincide with a buildings construction types and systems (U.S. Department of Energy, 2018a). This study examined the use of EnergyPlus™ for the purpose of modeling low income housing in developing countries, and investigating methods for validating these models based on sparsely monitored test houses, in order to make energy efficiency suggestions for existing and future homes.

This research is a continuation of a long-term study begun in 2011 by Ramsdell, Delarm Neri, Jacobs, & Verster (2012), at the University of the Free State in South Africa. Ramsdell and his colleagues focused on housing built through a government subsidized housing program in South Africa known as the Reconstruction Development Program (RDP) (Ramsdell et al., 2012). In the first phase of this study, the research team set out to show that it is possible, through simple and cost-effective efficiency upgrades, to drastically reduce a building's heating energy use in colder months, and to improve occupant comfort year-round (Ramsdell et al., 2012). This was done through the use of BEM software, by modeling the test houses as built, and comparing these models to those same houses as modeled with a number of simple energy efficiency upgrades (Ramsdell et al., 2012). Furthermore, the researchers conducted life cycle cost analyses to show the payback period in energy savings of each efficiency measure. The results from the first phase of the study show that there is the potential for a large reduction in energy use with the implementation of the suggested building efficiency measures (Ramsdell et al., 2012). The majority of the efficiency measures also showed a financial benefit over the proposed 30-year lifespan of the building (Ramsdell et al., 2012).

In the second phase of this study, HOBO® data loggers were installed in the houses that were modeled in the first phase, in order to record interior and exterior conditions including temperature and relative humidity, so as to compare actual conditions to those present in the models. Upon comparison of the measured interior temperatures versus the predicted interior

temperatures produced by the BEM, a relatively close correlation between the two was found, except for in the cold months of the year (Ramsdell et al., 2012). Upon further investigation into the inner workings of how EnergyPlus™ models the conditions in question, it was found that the model assumes that the air in the thermal zones is well mixed, which may not be the case for the zone conditions in the houses being monitored in South Africa. This may account for some of the discrepancies in actual temperatures compared to those that the model predicted, based on where the HOBO data loggers were placed in relation to heat sources.

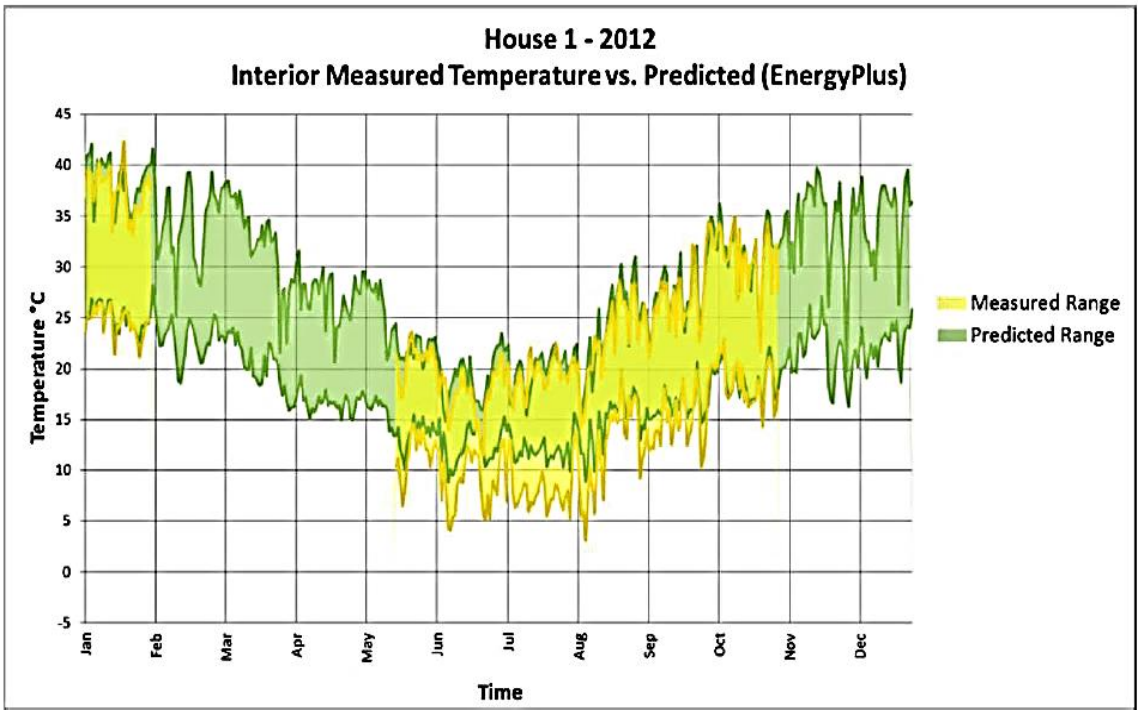

Figure 1. Comparison of recorded interior temperatures to those predicted by EnergyPlus™ simulation using AMY data (Ramsdell et al., 2012, p. 1025).

The HOBO data loggers were installed in each house at a wall height of approximately seven feet. The houses which were examined in this study were all constructed with the following features: "concrete strip footings, masonry walls of clay brick or concrete block, pitched roof with corrugated metal or concrete tile roofing, concrete floor with ceramic tile or

no finish, timber or steel" (Ramsdell et al., 2012, p. 4). Given the loose nature of the construction of the houses studied, and the position of the loggers relative to the heat source in each house, one might suspect that these houses are subject to high levels of thermal stratification, and that the data loggers were placed in an area where the average temperature did not coincide with the well-mixed average zone temperatures that the EnergyPlus™ model assumes. Given the discrepancies between the collected data and the outputs from the EnergyPlus™ model, it would be difficult to make meaningful energy conservation recommendations regarding the construction methods and assemblies used, when the recommendations are based on a model that does not accurately depict temperatures felt by the occupant or realistic heating energy use and heater run times. Considering this, it was necessary to find a method for modeling these structures in the software that accounted for thermal stratification, which might give a more accurate picture of temperatures felt by the occupants in these structures, and the amount of heat energy required to maintain a certain heating setpoint.

In EnergyPlus™ there are input objects that allow for the examination of non-uniform zone air temperatures, a feature known as Room Air Models (U.S. Department of Energy [USDOE], 2018a). These inputs were designed to model air temperature distributions in displacement ventilation systems, in conjunction with other air-side controls (OpenStudio, 2018). In the model, however, when there are no mechanical ventilation systems as inputs, the model will simply generate outputs for the temperatures at three different node heights (USDOE, 2018a). The specifics of how these measures are programmed and implemented will be discussed in detail later in this paper.

Purpose of the Study

The purpose of this study was to develop a method for validating energy models for buildings with no forced air, that utilize simple construction techniques, and that are sparsely monitored, in order to make suggestions for energy efficiency improvements for low income

residences in both developed and developing nations. If there is good agreement between the baseline energy model and measured data, then it will be possible to make better predictions about energy use based on existing construction techniques. If accurate predictions can be made for energy use and the occupied zone temperatures in residential buildings constructed with inefficient air sealing and insulation methods, then suggestions can be made about methods for increasing building energy efficiency and thereby occupant comfort. It might also be possible to show that up-front costs in building components and techniques are justified by the overall reduction in residential energy use that they may afford. If any amount of future energy use can be avoided through efficiency measures, then it may be possible to avoid some percentage of future production of greenhouse gases, in turn mitigating some of the effects of climate destabilization.

Research Questions

1. Is there thermal stratification in buildings with loosely constructed envelopes and no centralized forced air system in the heating season?
2. To what degree of accuracy does the Room Air Model predict actual temperature measurements in buildings with loosely constructed envelopes in which there is no centralized forced air system?
3. To what degree of accuracy does the Room Air Model's predicted temperatures match the interior zone temperature data that has been collected in the previously-cited South Africa research?

Hypothesis

The EnergyPlus™ Three-Node Displacement Ventilation RoomAir Model will predict the temperature profiles in the test building used in this study with approximately 10% error.

Limitations of the Study

One limitation of the study was the use of the Three-node Displacement Ventilation (DV) RoomAirModel in EnergyPlus™, which is the only simplified modeling method available to examine multiple temperature gradients over a building's height. This measure is intended for use in models that are simulating buildings that utilize a ducted ventilation strategy, whether mechanical or natural, known as displacement ventilation. The energy models examined in this study simulated homes that have no duct work, and as such are provided fresh air only by the natural air changes that are a result of loose construction and fenestrations.

Another limitation to this study was the fact that the houses that were modeled in South Africa were sparsely monitored, and thus we had to assume they were subject to high levels of thermal stratification. A test building that was available for use was modeled in the experimental portion of this research, but the construction assemblies used in the building are considerably different than those used in the houses in South Africa. In the test building it was necessary to simulate thermal stratification through manipulation of air changes and heat sources in the building. While the building construction assemblies present in the test building were very different from those used in the houses in South Africa, if the modeling approach is accurate in its predicted interior conditions of the building in question, then the approach should be applicable to other buildings that are subject to high levels of infiltration.

The last limitation was that the only heat gain that was placed in the building was an oil-filled radiant heater. In the DV RoomAir Model in EnergyPlus™, the gains that are examined are typical of an office setting, and a consistent heat gain input is needed for the model to function as intended. This will be further discussed later in this paper.

Significance of the Study

This study was intended to add to the existing body of knowledge regarding building energy modeling methods; more specifically, modeling homes with loosely constructed envelopes and poorly executed insulation. Previous studies have been done on validating the use of the Room Air Model in EnergyPlus™, but as was stated previously, the buildings examined in these studies had ducted ventilation systems. To the author's knowledge, there have not been, as of yet, any studies that examined thermal stratification in loosely constructed buildings. It is the hope of the author that this research will provide some insight into the modeling of buildings using more rudimentary methods, and anyone interested in methods for reducing energy use and improving occupant comfort in low income residences.

CHAPTER 2: REVIEW OF LITERATURE

Thermal Stratification

According to Linden (1999), air flow in buildings is generated naturally through the forces of wind acting on the outside of the building, and through buoyancy that is a result of temperature differences between the outside and the inside of the building. These buoyancy forces can lead to thermal stratification in the interior of the buildings. The presence of this thermal stratification in the building's interior can lead to very different air flow patterns than those seen in buildings with well-mixed air (Linden, 1999).

In the case of buildings that are utilizing natural ventilation for conditioning the interior of the space, the amount of thermal stratification in the space is dependent upon the location of the ventilation openings (Linden, 1999). If there is a single opening located high in the space, there will be an exchange of cool air coming into the space, while warm air exits the space. The incoming cool air will descend into the space, mixing with the existing air in the space as it falls (Linden, 1999).

In spaces that have two openings for ventilation, one high and one low, warm air will exit the space through the upper opening, while cool air will enter through the opening located lower in the space. When used deliberately for conditioning a space, this method is known as displacement ventilation, and is characterized by high levels of thermal stratification (Linden, 1999).

This method can be used to effectively maintain occupant comfort in buildings with well executed air sealing during the cooling season. However, during the heating season, buildings with poorly executed air sealing can be subject to this phenomenon as well. One of the

predictions made in this paper is that due to the loosely constructed envelopes of the buildings in the South Africa research conducted by Ramsdell et al. (2012), during the heating season much of the heat generated in the spaces by heating appliances is escaping through the upper portion of the building's envelope, drawing in cold air from lower portions of the building's envelope and resulting in high levels of thermal stratification, leading to a low level of occupant comfort in the occupied zone in the space.

According to Linden (1999), when the space inside a building is warmer than the exterior ambient temperature, there is a height in the space at which the internal pressure is equal to the exterior air pressure. This height is known as the neutral level (Linden, 1999). Below this level the pressure is lower than the ambient pressure, and above this level the pressure is higher than ambient pressure. This pressure difference is what drives airflow in and out of openings in the building, with air flowing out of the building's openings at heights higher than the neutral level, and in through openings lower than the neutral level (Linden, 1999).

Displacement Ventilation Systems

Displacement ventilation (DV) is a ventilation technique that uses low velocity conditioned air introduced at or near floor level, which minimizes mixing of air in the space, and induces a vertical temperature gradient (American Society of Heating, Refrigerating and Air-Conditioning Engineers [ASHRAE], 2019). As ventilation air enters the space it is entrained into convective thermal plumes that have been generated through the effects of buoyancy and heat gains from equipment and occupants in the space (ASHRAE, 2019). As a thermal plume rises, it begins to expand as air surrounding the plume is entrained, generating what is commonly referred to as a top hat profile (ASHRAE, 2019). According to the ASHRAE Handbook HVAC Applications Guide (2019), the velocity and growth of the thermal plume are directly related to the size of the heat gain, and the ambient temperature around the load. As the air rises in these thermal plumes, it is then displaced by cooler fresh ventilation air below (ASHRAE, 2019).

There is a height at which the plume will begin to expand and mix with other thermal plumes in the space, forming a clearly definable layer between an upper mixed zone and a lower occupied zone (ASHRAE, 2019). It is in the upper mixed zone where the warm stale air is removed through the exhaust along with pollutants generated by the occupants (ASHRAE, 2019). The layer between the upper mixed zone, and the lower occupied zone is referred to as the neutral level (Linden, 1999). The neutral level, or neutral height, is determined based on the relationship between the velocity of the incoming air , and the size of heat gains in the space (ASHRAE, 2019).

To avoid cooling the occupants, the incoming ventilation air is introduced at rates somewhere between 40-70 ft/min, and generally above 60 °F, rates that are slower and warmer than those seen in typical HVAC systems (ASHRAE, 2019). Because of this, DV systems are typically more energy efficient than more commonly used HVAC systems (ASHRAE, 2019).

Modeling Thermal Stratification in Displacement Ventilation Systems

There are four different methods for modeling thermal stratification in zones that utilize displacement ventilation: multilayer plume equation-based models, nodal models, semi-empirical experimentally based models, and computational fluid dynamics (CFD) (da Graça, 2003). The use of CFD to model these systems is very computationally expensive and requires a high level of expertise to produce models that are accurate (da Graça, 2003). In a nodal model produced by Rees and Haves (2001), the use of pre-calculated rates for airflow produced through experimentation and CFD, followed by the mathematical application of energy conservation to the model, were shown to be successful in predicting air flow and temperature profiles. However, this approach does not model thermal plumes in the space, which are essential to the successful design of displacement ventilation (DV) systems (Rees & Haves, 2001). Although semi-empirical experimentally based models have provided a great deal of insight into the evaluation of the fundamental mechanisms behind displacement ventilation

systems, they are lacking in their capability to model complex room geometries and real-world scenarios (Mundt, 1996).

The mathematical models used in the energy modeling software that is examined in this paper are an extension of mathematical models that were developed to simulate the physical principles of DV systems by Linden, Lane-Serff, and Smeed (1990), and Morton, Taylor, and Turner (1956). The multi-layer plume equation-based models examined in these works, as was stated previously, only examine plume flows, which is the driving force behind the principles of DV systems (Linden et al., 1990; Morton et al., 1956). The scenario that was modeled in the previously mentioned works was for a single plume in a zone with adiabatic walls, making this model somewhat limited in its applicability to real world scenarios (Linden et al., 1990; Morton et al., 1956). The model produced by da Graça (2003) was an attempt to overcome the limitations inherent to this particular model, creating something that is applicable for zones with non-adiabatic walls that house multiple thermal plumes.

In their work *Empty Filing Boxes: The Fluid Mechanics of Natural Ventilation*, Linden et al. (1990) used scaled models and salt water to simulate the effects of buoyancy on air flows in a naturally ventilated structure by varying water density levels through changes in water salinity. This work showed that in a constantly ventilated adiabatic box housing a single plume, two layers formed (Linden et al., 1990). The lower layer that formed had a similar air temperature and density to the fluid entering the box, and the upper layer had a similar temperature and density to the fluid leaving the box (Linden et al., 1990). This work also showed that the dividing point of the two different density layers of fluid in the space occurred where the flow rate of the plume was equal to the flow rate of the incoming fluid (Linden, et al., 1990). The ability to be able to predict this height is the most important aspect of modeling thermal stratification in DV systems, because when this interface between the warmer upper

mixed layer and the cooler lower layer occurs in the occupied zone, the cooling capabilities of the system are diminished or altogether lost (da Graça, 2003).

There are a number of factors that play a part in maintaining the desired height of the neutral level in a zone. When the heat flux generating a thermal plume is increased by an order of magnitude, it can have the effect of reducing the neutral height by one third (da Graça, 2003). This is important to note when attempting to model zones that have a high heating load, in which a heater will be cycling on and off according to interior conditions, as was being done in this study. Similarly, when the incoming air flow rate is reduced by half, it can again reduce the level of the neutral height by one third (da Graça, 2003). This is another important issue to note regarding the models in this experiment, in which the only air flow was from infiltration and inter-zone airflow. In the design of DV systems, these variables need to be in a relatively precise range in relation to one another in order to maintain the simplicity and energy efficiency of the system (da Graça, 2003). The conditions used in the experimental procedures of this study for these two factors, size of the heat gains in the space and the amount of air flow, are what led to the inconclusive results that will be discussed later in this paper.

Linden and Cooper (1996) found that the modeling approach for scenarios in which there is a single plume is also applicable in scenarios where there are multiple plumes of equal strength, due to the fact that in both scenarios two layers are generated, with the largest variations in temperature taking place between the lower and upper layer. In the work by da Graça (2003), scenarios with multiple equal strength plumes, as well as multiple variable strength plumes, were examined. It was found that when there are multiple plumes of varying strength, a separate layer is formed in the space for each of the plumes that are present (da Graça, 2003). Under these circumstances, the methods for predicting the transition between layers was still found to be applicable, occurring at the point where the plume flow rate for each plume matched the flow rate of the incoming air. It was further discovered that when multiple

plumes are present, the flow from equal strength plumes is always higher than that of unequal plumes at a given height (da Graça, 2003). For the sake of modeling, it was necessary to find a method that is simple and the most widely applicable. For this reason, da Graça (2003) examined the outcome of applying the mathematical model for multiple equal strength plumes, to scenarios in which the plumes were of varying strengths. It was found that when modeling two and three asymmetric plumes, the model results were conservative (da Graça, 2003). The results from the model showed an underestimation of the height at which the neutral level is located, as well as an underestimation of the temperature transition, with the largest temperature changes occurring higher than what the model predicted (da Graça, 2003). In another scenario in which nine symmetric plumes were present, with one larger plume, it was found that the model was overly conservative (da Graça, 2003). The model results showed that the largest temperature change took place lower than what was observed, leading potential designers to believe that the largest plume would play a role in the temperature in the occupied zone (da Graça, 2003). This led da Graça (2003) to conclude that in scenarios where there are multiple plumes of equal strength, and one larger plume, the equal plume method is not appropriate, but the two plume method is applicable when the larger plume, as well as all of the smaller plumes grouped into one, are used.

The doctoral dissertation by da Graça (2003) also advised on a number of scenarios in which the multilayer plume equation-based model should not be used, which will be discussed later in this paper. It is up to the user to determine the appropriateness of the modeling method being applied in a given instance. The conditions under which other methods of modeling should be used follow:

- When heat flux from internal gains is matched by heat flux in the lower layer from the floor or the walls (da Graça, 2003).

- When buoyancy flows driven by the ceiling, the floor, or the walls are of the same order of magnitude as the plume driven flows from internal gains (da Graça, 2003).
- When there is positive or negative buoyancy from the floor, which can disrupt internal gain driven plume flow, even when it is the dominant source of flow (da Graça, 2003).
- When there is enough heat flow across the ceiling construction assembly to the exterior that the uppermost region of the mixed layer becomes significantly cooler than the rest of the mixed region (da Graça, 2003).

Another factor that introduces additional complexity into the problem of modeling DV systems is the distribution of gains in the space. For the sake of simplicity, all internal gains that produce plumes are viewed as having a point source of origin at the floor level (da Graça, 2003). In situations where an occupant has multiple pieces of equipment at their desk (computers, task lighting, etc.) all within .5 m of one another, based off of experiments performed by Kaye and Linden (2003), it is reasonable to view the occupant and the surrounding pieces of equipment as a single source of plume generation. Using this approach, the modeler can divide the total of the convective gains in the occupied zone by the total occupants in that same space in order to find the average power of the gains in each plume (da Graça, 2003).

The last thing that is important to take into consideration when modeling internal gains in a space is how the gains are distributed vertically (da Graça, 2003). According to da Graça (2003), "whenever the thermal plumes are the sole buoyancy sources in a room the heat in these sources is totally convected into the upper warm layer" (da Graça, 2003, p. 196). However, it is typical in real world scenarios for there to be other factors that will impede 100% of the heat in a thermal plume from reaching the upper mixed layer. Some of the factors listed by da Graça (2003) include: plume interference from furniture, interference from wall driven layers that are negatively buoyant, and floor driven positive buoyancy (da Graça, 2003). One

will often find in an office setting that there are sources of heat gain in a space located under furniture, such as the tower for a desktop computer. In this instance, the plume flow generated by heat gain from the computer is disturbed by the desk, and as such part of the heat generated by the computer must be accounted for in the occupied zone when attempting to model heat and airflow in the space (da Graça, 2003).

For this reason, da Graça developed a means of accounting for the convective gains from the thermal plumes in the lower layer by incorporating a fraction of the total gains into the energy balance for the occupied zone. In the model this fraction of gains is denoted by *FRg* (da Graça, 2003). This value will be between one and zero. In instances where a large open space in which the gains are primarily from people and equipment rather than solar gain, this value should be on the lower end, somewhere close to zero (da Graça, 2003). In a small room in which there are many objects and pieces of furniture, this value will be considerably higher (da Graça, 2003). The *FRg* is multiplied by the heat gain in the calculation, and then incorporated into the calculation for the occupied sub-zone temperature (da Graça, 2003).

In a later study performed by Mateus and da Graça (2015) on the validation of the methods reviewed here, multiple model runs were performed with the value for the fraction of heat gains in the occupied zone varying between zero and one, in order to obtain a best fit for this value. The authors found that a value of 0.4 led to the lowest percentage of error (Mateus & da Graça, 2015). The value found here was the same as that found in a study performed using CFD simulations for a concert hall by the same authors (Mateus & da Graça, 2015). When applying this value to the models examined in this study, the results led to more unexpected outcomes, which are likely a result of a combination of other inputs in the model. This issue will be discussed later in this paper.

EnergyPlus™ RoomAir Models

The methods developed for modeling thermal stratification and neutral height in DV systems that have been reviewed in this paper were implemented in the energy modeling software EnergyPlus™, in the model group referred to as RoomAir Models (U.S. Department of Energy, 2018a). The single node fully mixed method of modeling room air temperature that is typically used in energy simulation software was adapted to a three-node model which allows the user to examine temperature profiles in DV systems with a first order of precision accuracy (U.S. Department of Energy, 2018a). A framework was developed by Griffith and Chen (2004) in order to couple building load and energy calculations to building energy models that are intended to examine complex air flows in thermal zones. This framework was altered for use in EnergyPlus™ in order to examine building energy use on an annual basis rather than just an hourly one, and to perform load and energy use calculations based on present mean air temperature, rather than on the temperature setpoint (U.S. Department of Energy, 2018a). The resultant formula examines heat transfer from gains inside and outside of the building, and across the building envelope, in order to determine the temperature of surfaces inside the zone at each time step (U.S. Department of Energy, 2018a).

$$T_{s_{i,j}} = \frac{T_{so_{i,j}} Y_{i,o} + \sum_{k=1}^{nz} T_{so_{i,j-k}} Y_{i,k} - \sum_{k=1}^{nz} T_{s_{i,j-k}} Z_{i,k} + \sum_{k=1}^{nq} \Phi_{i,k} q"_{ki_{i,j-k}} + T_{a_{i,j}} h_{c_{i,j}} + q"_{LWS} + q"_{LWX} + q"_{SW} + q"_{sol}}{Z_{i,o} + h_{c_{i,j}}} \quad (1)$$

Where:

T_s represents the inside face temperature

i represents the subscript for individual surfaces

j represents the current time step

k represents the time history steps

T_{so} represents the outside face temperature

Y_i represents the cross CTF coefficients

Z_i represents the inside CTF coefficients

φ_I represents the flux CTF coefficients

q''_{ki} represents the conduction heat flux through the surface

h_{ci} represents the surface convection heat transfer coefficient

T_a represents the near-surface air temperature

q''_{LWS} represents the longwave radiation heat flux from equipment in the zone

q''_{LWX} represents the net long wavelength radiation flux exchange between zone surfaces

q''_{SW} represents the net short wavelength radiation flux to surface from lights

q''_{sol} represents the absorbed direct and diffuse solar radiation

As was mentioned earlier, the UCSD DV model was developed by da Graça (2003), in order to create a method of modeling displacement ventilation systems in spaces with complex geometries, housing multiple plumes, with non-adiabatic walls. The assumptions of the model produced by da Graça (2003) are as follows:

- All plumes generated in the space are equal in strength (da Graça, 2003).
- All plumes are viewed as located in the floor of the zone, and as "point sources of buoyancy" (da Graça, 2003, p. 200).
- Convective currents generated by surfaces in the zone are not taken into consideration (da Graça, 2003).
- "Heat transfer from each individual surface is evaluated using natural convection correlations" (da Graça, 2003, p. 200).
- Each room surface is coupled to its corresponding subzone, and when there are multiple zones in which a surface is located, a weighted area is used to account for heat transfer into the zone (da Graça, 2003).

- The plume buoyancy flux in the zone is modeled by adding all of the internal gains that are in the occupied zone together and dividing by the number of plumes (da Graça, 2003).

In order to characterize the stratification in a zone, the model predicts three temperatures that correspond with the three different levels that form in a zone served by a DV system:

1. The temperature in the floor zone, noted by T_{floor}, which accounts for any heat transferred from the floor into the incoming supply air.
2. The temperature in the occupied zone, noted by T_{oc}, representing the temperatures experienced by the zone occupants.
3. The temperature in the upper mixed zone, noted by T_{mx}, which corresponds with the temperature in the zone where pollutants and warm air are mixed above the occupants, as well as the exhaust air.

The model begins by calculating $\dot{Q}$, which is the sum of all the internal convective heat gains located in the occupied zone, and then dividing this value among the number of plumes in the zone. According to the U.S. Department of Energy EnergyPlus™ 9.2 Input Output Reference (2018a), the heat gains listed in the occupied zone are as follows: people, electric equipment, task lighting, hot water equipment, gas equipment, steam equipment, other equipment, and baseboard heat (U.S. Department of Energy, 2018b). Gains in the mixed zone are also taken into consideration in the calculations and include: high temperature radiant heaters, general lights, and tubular daylighting devices (U.S. Department of Energy, 2018b). The calculations for convective heat transfer in the zone are as follows:

$$\dot{Q}_{\text{ocz}} = \dot{Q}_{\text{oc,conv}} + \dot{Q}_{\text{tl,conv}} + \dot{Q}_{\text{eleq,conv}} + \dot{Q}_{\text{gaseq,conv}} + \dot{Q}_{\text{otheq,conv}} + \dot{Q}_{\text{hw,conv}} + \dot{Q}_{\text{stmeq,conv}} + \dot{Q}_{\text{bb,conv}} \quad (2)$$

$$\dot{Q}_{\text{mxz}} = \dot{Q}_{gl,conv} + \dot{Q}_{ltp} + \dot{Q}_{htrad,conv} \quad (3)$$

$$\dot{Q}_{tot,conv} = \dot{Q}_{ocz} + \dot{Q}_{mxz} \quad (4)$$

Where:

$\dot{Q}_{\text{ocz}}$ is the total heat gain in the occupied zone

$\dot{Q}_{\text{oc,conv}}$ is the general convective heat gain in the occupied zone

$\dot{Q}_{\text{tl,conv}}$ is the heat gain from task lighting

$\dot{Q}_{\text{eleq,conv}}$ is the heat gain from electric equipment

$\dot{Q}_{\text{gaseq,conv}}$ is the heat gain from gas equipment

$\dot{Q}_{\text{otheq,conv}}$ is the heat gain from other equipment

$\dot{Q}_{\text{hw,conv}}$ is the heat gain from hot water equipment

$\dot{Q}_{\text{stmeq,conv}}$ is the heat gain from steam equipment

$\dot{Q}_{\text{bb,conv}}$ is the heat gain from baseboard heating

$\dot{Q}_{\text{mxz}}$ is the total heat gain from the mixed zone

$\dot{Q}_{gl,conv}$ is the heat gain from general lighting

$\dot{Q}_{ltp}$ is the heat gain from tubular lighting devices

$\dot{Q}_{htrad,conv}$ is the heat gain from high temperature radiant heaters

Next the model calculates the supply air flow rate which is denoted by $\dot{V}$ (U.S. Department of Energy, 2018a). The air flow rate into the zone considers all of the following: infiltration, supply air, inter-zone flow, and ventilation air (U.S. Department of Energy, 2018a). The calculations for the supply air flow rate are as follows, where MCP is the rate of mass flow

multiplied by the specific heat capacity of air, and MCPT represents the rate of mass flow multiplied by specific heat times the air temperature:

$$MCP_{zone}=MCP_i + MCP_{vent} + MCP_{mix} \quad (5)$$

$$MCP_{sys} = \sum \text{inlets}\, \dot{m}_i C_{p,i} \quad (6)$$

$$MCP_{tot} = MCP_{zone} + MCP_{sys} \quad (7)$$

$$MCPT_{zone} = MCPT_i + MCPT_{vent} + MCPT_{mix} \quad (8)$$

$$MCPT_{sys} = \sum \text{inlets}\, \dot{m}_i C_{p,i} T_i \quad (9)$$

$$MCPT_{tot} = MCPT_{zone} + MCPT_{sys} \quad (10)$$

Where:

$\dot{m}_i$ is the mass flow rate

C_p is the specific heat

The user is required to input the number of occupants, $N_{occ,\, the}$ number of plumes per occupant, $N_{plumesperpers}$, and the percentage of the internal convective heat gains that remain in the occupied zone, Fr_{gains}, not to be taken into consideration in the thermal plumes in the zone. These inputs are represented by the following equations:

$$N_{plumes} = N_{occ} \cdot N_{plumesperperson} \quad (11)$$

$$\dot{Q}_{\text{plumes}} = (1 - Fr_{gains}) \cdot \dot{Q}_{tot,conv} \quad (12)$$

$$\dot{Q}_{\text{perplume}} = \dot{Q}_{\text{plumes}}/\text{N}_{\text{plumes}} \quad (13)$$

Using the aforementioned user inputs, the model then makes its initial estimate of the neutral height in the zone, or the height of the boundary layer Fr_{hb}, which is calculated as a fraction of the total ceiling height. Here MCP_{tot} is converted to a volumetric flow rate using $1/(\rho * c\rho air)$= 0.000833 (U.S. Department of Energy, 2018a).

$$Fr_{hb} = \left(\frac{24.55}{H_{ceil}}\right)\left(\frac{0.000833 \times MCP_{tot}}{N_{plumes} \times \dot{Q}_{perplume}^{\frac{1}{3}}}\right)^{\frac{3}{5}} \quad (14)$$

Following the initial estimate of the boundary layer height, the iterative solver calculates the heat transfer coefficient, and a temperature for each surface in the zone, taking into consideration the subzone in which each surface is located (U.S. Department of Energy, 2018a). Once the heat transfer from the surfaces in each subzone can be coupled with the air flows and heat gains in that subzone, the model recalculates the boundary layer height, followed by the three subzone temperatures (U.S. Department of Energy, 2018a).

The calculations in the iterative solver initially assume that the air in the zone is thermally stratified when the Three Node DV RoomAir Model is applied (U.S. Department of Energy, 2018a). In the model there are checks in place to verify that the RoomAir Model was appropriately applied given the specified heat gains and air flows in the zone, and that the air in the zone is in fact thermally stratified (U.S. Department of Energy, 2018a). If one of the following conditions is true, then the model will perform the zone calculations again with the assumption that the air in the zone is well mixed:

- If the temperature in the mixed subzone is less than the temperature in the occupied subzone.
    - ($T_{mx} < T_{oc}$)
- If the total air flow rate MCP_{tot}, in the zone is less than or equal to 0.

- ($MCP_{tot} \leq 0$)

- If the height of the boundary layer, $H_{fr}*H_{ceil}$,is less than the total height of the floor zone and the occupied zone when added together, $H_{fl,top}+\Delta z_{occ,min}$.
  - ($H_{fr}*H_{ceil} < H_{fl,top}+\Delta z_{occ,min}$)

It should be noted that the minimum necessary change in height of the occupied zone is 0.2 meters, and the top of the floor zone is located at 0.2 meters.

The checks noted here will be discussed further in this paper, as some of the inputs from the experimental portion of this research which were used in the model were found not to be ideal in terms of the methods used in the model for calculating zone conditions.

Validating Building Energy Models

Displacement ventilation systems are designed to remove internal gains that are both radiative and convective. This means that the surfaces in a space that is being modeled also play a large role in the calculations due to the fact that they are being heated through radiative heat transfer, which in turn transfer heat to the air in the space. Because of this, the vertical temperature profile has a smoother transition than one might see in the profile from experiments that examine salinity concentration or CO_2 distribution (Mateus & da Graça, 2015).

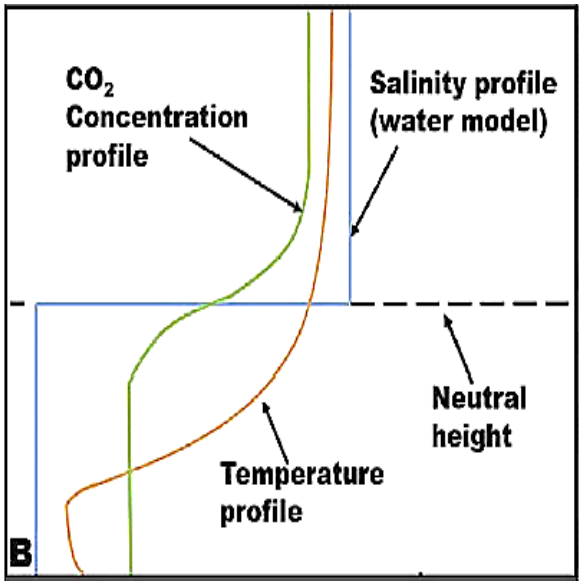

Figure 2. "Typical temperature, concentration and salinity profiles" (Mateus & da Graça, 2015).

According to Mateus and da Graça (2015), "Most DV application cases have a coincidence between heat and pollutant sources, resulting in a mixed layer region that contains the indoor pollutants and, therefore, should be kept above the occupants head height" (p. 50). Examination of the distribution profile of contaminant concentration shows a much more visible change in the gradient at the neutral height level compared to the gradient around the neutral height as seen in temperature profiles (Mateus & da Graça, 2015). This means that experiments that examine both contaminant distribution and temperature profiles can be used to verify the plume theory developed by Morton et al. (1956), which is the basis for the methods used to predict the neutral height in the EnergyPlus™ RoomAir Model for displacement ventilation (Mateus & da Graça, 2015).

The method created for defining the neutral height based on air temperature and pollution distribution profiles by Mateus and da Graça (2015) seeks to locate the neutral height by finding the height in the room above which the temperature gradient is much smaller than in

the rest of the room, based on the fact that in the lower occupied layer of the space the temperature increase is always much higher than in the upper mixed portion of the room (Mateus & da Graça, 2015). The method begins by assigning the average temperature gradient over the total height of the room the notation NTG, or normalized temperature gradient (Mateus & da Graça, 2015). This is equal to:

$$NTG = \frac{T_{zceiling} - T_{zfloor}}{Z_{ceiling} - Z_{floor}} \quad (15)$$

Where:

$T_{zceiling}$ is the temperature at the ceiling

T_{zfloor} is the temperature at the floor

$Z_{ceiling}$ is the height at the ceiling

Z_{floor} is the height of the floor node

Next, "all experimental temperature profiles are discretized using one hundred points spaced equally between the floor and ceiling; and a rolling average smoothing, with a ±0.1 m vertical averaging interval, is also applied to avoid false results due to local inflections in the experimental profiles" (Mateus & da Graça, 2015, p. 55). The method used by Mateus and da Graça (2015) then checks the temperature profiles to identify places in which the gradient is less than NTG by a factor which is produced with the following calculation:

$$(1 + C_{\mathrm{NH}}) \times \frac{T_{ztotal} - T_{z0}}{z_{total} - z_0} > \frac{T_z + 1 - T_z}{(z+1) - z} \quad (16)$$

Where:

C_{NH} is the neutral height in the contaminant profile

T_{ztotal} is the overall temperature change

T_{z0} is the initial temperature

Z_{total} is the total change in height

Z_0 is the initial height

T_z is a temperature at a given height

Z is a given height

The value that was used for the coefficient is Cnh =.3. To quantify the discrepancies found between the prediction of neutral heights between the methods, Mateus and da Graça (2015) use the following equations:

$$\text{Bias(m)} = h_{\text{temp.profile}} - h_{\text{contaminants}} \tag{17}$$

$$Error\ (\%) = 100\%\ x \left| \frac{h_{\text{temp.profile}} - h_{\text{contaminants}}}{h_{\text{temp.profile}}} \right| \tag{18}$$

Where:

h is the neutral height

After applying this method to a set of data gathered from previous studies that examined temperature profiles and contaminant distribution in displacement ventilation systems, an error of below 10% was found, while the average bias was very low at 4cm (Mateus & da Graça, 2015). Mateus and da Graça (2015) go on to use the previous method to evaluate the accuracy of calculating the neutral height using the mathematical model that was developed based off of the plume flow theory developed by Morton et al. (1956). When comparing the experimental neutral heights with those calculated using the mathematical model, it was found that the average error was 14%, with a correlation coefficient (R^2) of .69 (Mateus & da Graça, 2015).

Mateus and da Graça (2015) then go on to compare the model developed for the prediction of the temperatures in the three zones; mixed, occupied, and floor, to the measured

data in nine different cases from three studies. The predictions from the models were compared to the experimental data using the following methods for determining average error:

$$\text{Avg. Diff. (K)} = \frac{\sum_{i=1}^{9} |Simi - Measi|}{9} \tag{19}$$

$$\text{Avg. Bias (K)} = \frac{\sum_{i=1}^{9} |Simi - Measi|}{9} \tag{20}$$

$$\text{Avg. Error (\%)} = \frac{100\%}{9} \text{ x } \sum_{i=1}^{9} \text{ x } \left| \frac{Simi - Measi}{Meas.\max - Meas.min} \right| \tag{21}$$

According to Mateus and da Graça (2015), given the simplifications and assumptions that are made in the model, and the fact that in many of the studies experiments are performed in a nearly adiabatic test chamber, the results of the comparison are favorable. It was found that there was an average error of 5% in the simulations overall, which is roughly a 17% reduction in error from the model that does not account for mixing of inflow air with the room air (Mateus & da Graça, 2015). The largest errors were found at the floor level node at 6% (Mateus & da Graça, 2015).

CHAPTER 3: RESEARCH METHODS

This was a quasi-experimental study in which the dependent variables were the interior temperature, the degree to which there was thermal stratification present in the test building, and how well these matched the modeled results. The independent variable was the amount of heat and air flow introduced into the sample building to achieve thermal stratification and in turn provide the inputs for the BEM.

Once all thermal stratification experiments were conducted in the test structure, models of the building were run, and graphical representations were produced to compare different temperature profiles from the measured data to the temperature profiles produced by the modeling software.

Test Structure

The test building used in this experiment is located behind Katherine Harper Hall at Appalachian State University. The building was constructed using a shed roof design, with all building construction assemblies meeting or exceeding local code requirements. The building footprint measures 20' by 8' (Boyes, 2017). The foundation of the building consists of a set of CMU piers, and as such the floor is slightly elevated and exposed to exterior conditions, resting at approximately 2' off the ground (Boyes, 2017). The exterior of the south-facing wall is 9' tall, while the exterior of the north-facing wall is 7' tall (Boyes, 2017). This results in interior wall heights of approximately 8' and 6,' respectively. The north-facing wall was constructed with 2x6 studs located at two feet on center. The east and west walls were constructed using 2x4 studs located at 16" on center. The entrance door to the interior of the test building is positioned in the approximate center of the east-facing wall. The south-facing wall is a 2x4 double stud wall

which allows for an insulated cavity measuring 7.5" thick. The sheathing on the test building consists of 7/16" oriented strand board (OSB), with a layer of weather resistant barrier on all sides. The interior of the building is gypsum board on the walls and ceiling, and OSB on the floor.

Each of the walls in the test building is insulated with densely packed cellulose, which was performed using a method referred to as drill-and-fill (Boyes, 2017). According to the study performed by Boyes (2017), the cellulose was installed at a density of three pounds per square foot, which is around the minimum density to be considered dense packed cellulose.

Experimental Design

The purpose of this experiment was to simulate high levels of infiltration in a building during the heating season. The test building used in this experiment has an envelope that was very well constructed, meaning the building is well insulated and tightly sealed. For this reason, it was necessary to introduce a measurable amount of air into the building that correlated with a particular number of air changes per hour when measured at a 50 pascal (ACH@50) pressure difference between the inside and outside of the house. To do this, a custom blower door was built that would accommodate two Minneapolis Duct Blasters; one in the bottom of the door to introduce air flow into the building, and one in the top of the door to expel air from the building.

This experiment was conducted from early March to late April, 2019, during a period of time in which the weather conditions ranged from typical late winter weather to typical spring weather in the mountains, with temperatures ranging from 70 °F during the day to 20 °F at night. In this way we were able to examine the effects of thermal stratification in a building over a variety of exterior temperatures.

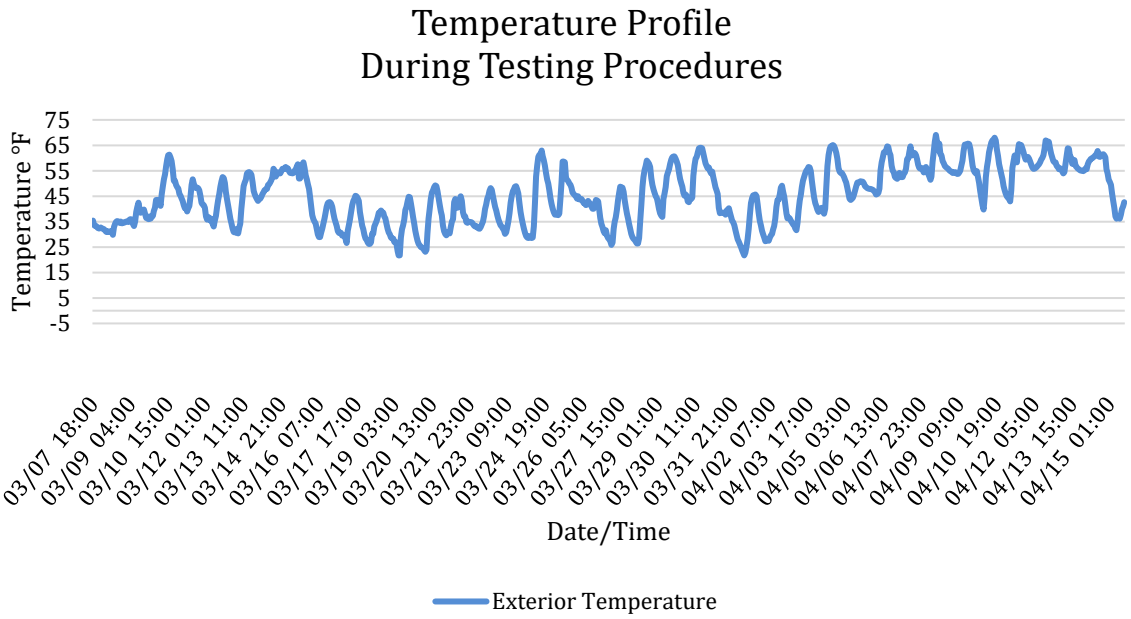

Figure 3. Exterior temperature profile over the course of experimentation.

A small radiant heater was used in the experiment, and sized so that the heat source would not overwhelm the interior of the test structure, theoretically allowing the potential for thermal stratification to take place. A network of temperature sensors, depicted in Figures 4 and 5, was hung from the ceiling on the interior of the building in order to measure the interior temperature profiles. To capture the exterior temperature profiles, a Vantage Vue weather station was set up adjacent to the building. There were three different treatments used in the experiment: (1) a baseline in which there was no air flow in the building, (2) one in which the air flow introduced into the building coincided with 5 ACH@50, and (3) one in which the airflow into the building coincided with 15 ACH@50. To allow for steady state conditions to develop, and to capture interior conditions that evolved with changing exterior weather conditions, each treatment that was applied was allowed to run between 12 and 48 hours.

Measurement Apparatus

Temperature sensor network.

In order to record the interior temperatures in the test shed over the course of the experiment, 42 Dallas 18B20 temperature sensors were hung at varying increments so that an accurate depiction of the temperature profiles in the room could be captured, taking into consideration the location of variables that would affect the temperature profile. These variables included location of the windows, the door, air inlet and outlet, any envelope penetrations, and the heat source. There were ten strands of temperature sensors in all. Nine of these strands were arranged in the space to capture the overall temperature profile. The last strand of temperature sensors was mounted on the interior of the blower door in order to capture the temperature of the cold air coming in from the exterior of the building, and the other to capture the temperature of the air after being heated as it exited the interior of the building. Images of the sensor network can be seen in Figures 4 and 5.

Figure 4. Temperature sensor network and radiant heater.

Figure 5. Temperature sensor network and custom blower door.

The nine strands of temperature sensors were arranged in three rows of three. Three different lengths of strand were used: one short, one medium, and one long. This was done in order to account for the change in ceiling height from one side of the interior to the other, because as was mentioned earlier, the building was constructed using a shed roof design. The short strands of temperature sensors were located along the shorter north-facing wall. Each of the short strands had three temperature sensors on it: one approximately 4” from the floor, one

at approximately 48", and one approximately 4" from the ceiling. The medium length strands of sensors were hung approximately 18" inches away from the south facing wall. These strands had seven temperature sensors on them: one at approximately 4" from the floor, one at approximately 48", and five sensors beginning at approximately 72" and continuing at 6" intervals up to the ceiling, the last terminating at approximately 4" from the ceiling. The location for the medium length temperature sensors is where it was estimated that the transition between the occupied zone and the mixed zone (or the interface height) would be most visible in the temperature profile based on the size of the space and location of factors that would affect the temperature readings such as windows and the door. The longest strands of temperature sensors were hung along the south-facing wall. Each of these strands had three temperature sensors on it: one at approximately 4" from the floor, one at approximately 48", and one at approximately 4" from the ceiling. Graphical representations for the method used to structure the placement and naming method for the sensors can be seen in Figures 6 and 7.

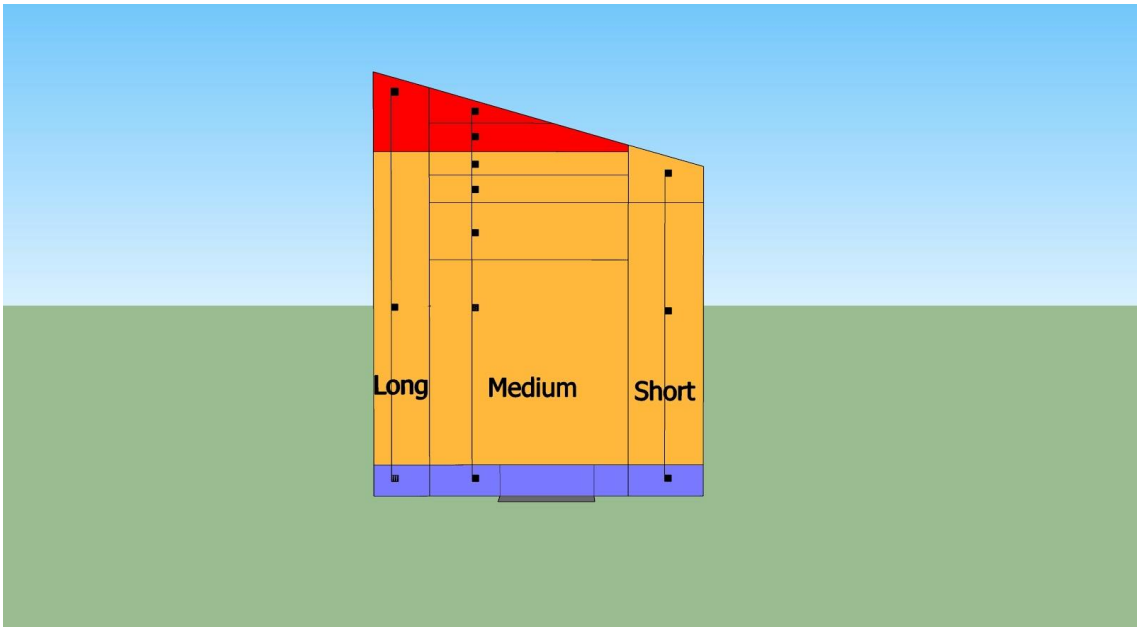

Figure 6. Temperature sensor network in section view.

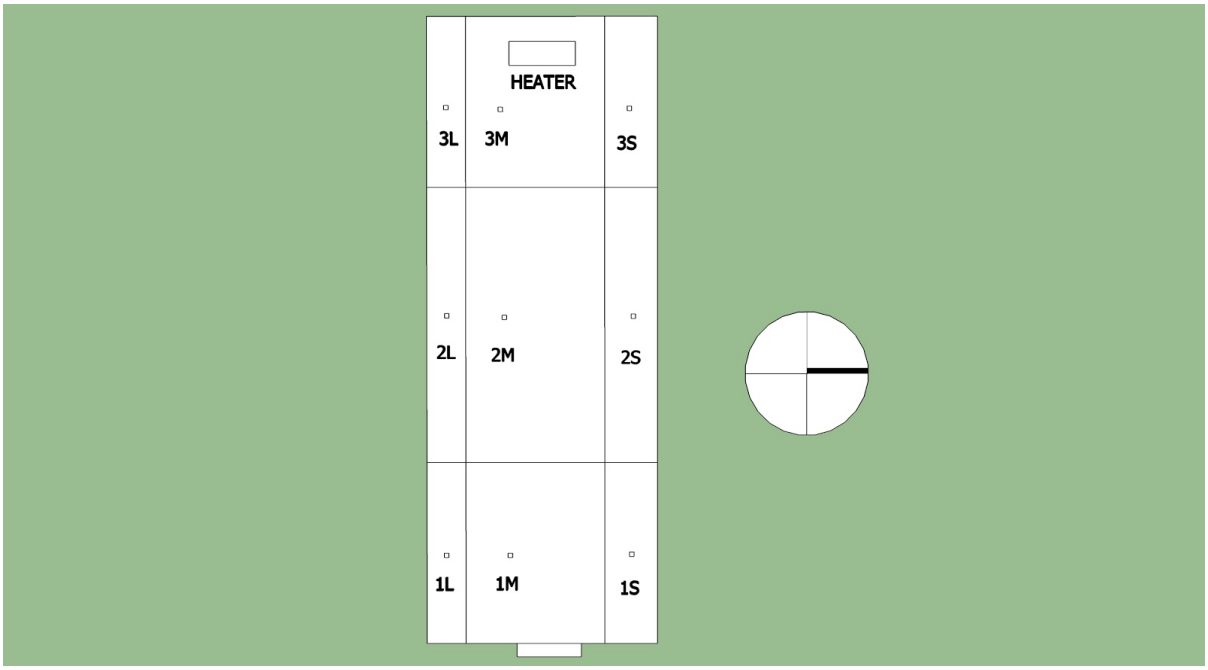

Figure 7. Temperature sensor network in plan view and location of radiant heater.

To capture the data that all of the sensors were collecting, the sensors were tied together at a breadboard that was hooked to a raspberry pi. The coding that was used for the readout of the data was done in Python. Three different Python modules were used for the data readout: one to record the time stamp, one to record the temperature reading, and one for export to a CSV file.

Zone heater.

The heater that was used in the earlier data collection in the experiment was a Honeywell Model HZ-709-WM. This heater has a rating of 12.5 Amps and operates on a standard 120 Volt outlet (ManualsLib, 2006). This heater utilizes electric resistance heating coils, which in turn heat oil inside the housing of the heater. The heater has three different heating elements, which operate in three different modes, depending on the setting of the heater (ManualsLib, 2006). The heater elements are rated as follows: small 600W, medium 900W, high or combined 1500 W. For this experiment, the heater was set to its highest setting,

1500 W. The heater is equipped with a digital display and controls that shows the room temperature, as well as the temperature setpoint on the heater. The heater has an automatic setting in which the desired temperature can be input and the heater will cycle on and off to maintain the desired setpoint. This was the setting under which the heater was operated for the purposes of this experiment. Unfortunately, about halfway through data collection for this experiment, the thermostat on the heater failed and a substitute heater was needed. The data collected from the run during which the heater failed was not used in the results.

The substitute heater that was used was a DeLonghi radiant heater, model EW6507L. This heater has the same basic setup, two electric resistance coils that are used to heat oil inside the heater housing (ManualsLib, 2004). However, this heater is not equipped with a digital display to control the temperature setpoint. This DeLonghi heater has two switches that can be used separately for a low or medium setting, or together for a high setting. The high setting was used in this experiment. Because this heater has no digital temperature control, a separate temperature controller was wired to the heater in order to maintain a consistent temperature setpoint in the space during the remaining data collection in the experiment. The temperature controller that was used was an Inkbird ITC-1000F.

Simulated infiltration/exfiltration.

In order to simulate the infiltration and exfiltration in a loosely constructed envelope, two Minneapolis Duct Blasters were attached to a custom-made blower door assembly. A picture of the door can be seen in Figure 8.

Figure 8. Custom blower door and Minneapolis Duct Blasters.

The blower door constructed for the purposes of this experiment used the same dimensions as the pre-hung door that was initially installed on the test building. The dimensions are as follows: 80” tall, 36” wide, and 1.63” thick. The door had three holes cut through it, each with an approximate diameter of 11”, for attaching the flange of the duct blaster duct termination to the door. The upper hole is approximately 10” to the center from the top of the door. The bottom hole is approximately 10” to the center from the bottom of the door. The door frame was made using pressure treated pine 2x4s cut to the appropriate dimensions. The frame was sheathed with ¼” plywood on the inside and ½” pressure treated plywood on the

exterior. The door was insulated using a layer of ¾" extruded polystyrene foam, as well as low expansion polyurethane spray foam to seal any remaining voids.

The smallest ring available with the duct blaster that was used for this experiment was a number three, which would not restrict the airflow enough to reach the desired number of air changes at the lowest setting available on the duct blaster fan. The lowest air flow that is achievable with the duct blaster, according to the reading on the DG-700, is 22 cfm. For this reason, it was necessary to create custom duct blaster rings. This was done using the existing rings and covering the hole of the duct blaster ring with a piece of foam core board, with the appropriately sized hole cut out in the center. Using a Lawrence Berkeley Laboratory Factor (LBL) of 20 in order to convert ACH @ 50 pascals to natural air changes per hour (ACHn), it was determined that a flow of 13.3 cfm would be needed to achieve 15 ACH@50, and a flow of 4.43 cfm would be needed to achieve 5 ACH@50.

Using the fan affinity laws that state there is a direct relationship between the diameter of an air flow orifice, and the corresponding mass that can flow through that inlet given a constant pressure difference, it was determined that the corresponding diameters that were needed to achieve the desired flow of 4.44 cfm for an ACH of 5, and 13.3 cfm for an ACH of 15, were .78" and 1.65" respectively (Fan Affinity Laws, 2003).

OpenStudio®/EnergyPlus™ Model of the Test Building

The parameters used for the OpenStudio® model of the test building that was used in this experiment are the same as described in the previously-given description of the physical building.

In order to produce accurate results in the model, it was necessary to create a custom EnergyPlus™ weather file (EPW). To do this a weather file from Boone, N.C. was used, and the existing data for portions of time during which the experiment was being conducted were overwritten using the data that was collected from the Vantage Vue weather station. The

parameters that were overwritten were the dry bulb temperature and the humidity. This was done using the application called Elements. In this program you can alter one variable such as dry bulb temperature keeping two other variables constant that you may want to also alter later, and the remaining variables will be changed based on the inputs according to the values on the psychrometric chart. In this way a weather file with actual data for temperature and relative humidity from the time period during the experiment was created, while the remaining values on the weather file were realistic in accordance with their interrelationship with the altered variables on the psychrometric chart.

It was discovered that the radiant convective electric baseboard heater that is in the HVAC component section of OpenStudio® is not the same as the baseboard heater that is accounted for in the internal gains of the Three-Node DV model. For this reason, OpenStudio® was unable to account for a scalable baseboard heater that is controlled by a thermostat tied to the interior temperatures in the building model zone. For this reason, it was necessary to revert to using only the EnergyPlus™ interface, which allows for more customizable user inputs. The baseboard heater that is in the EnergyPlus™ Three-Node DV model internal gains section is controlled by a thermostat that is tied to the exterior temperatures in the model. Through the use of the EnergyPlus™ Energy Management System (EMS), it was possible to create additional components in the model that allowed for this baseboard heater to be scalable in terms of allowable power input, as well as being controlled by a thermostat that is directly tied to the interior temperatures in the models.

Data Analysis Procedures

Research Question 1 Data Analysis Procedure

Once the temperature data and associated air flows were gathered from the test building, the temperature profiles in the data were then examined in order to gain an understanding of the air temperature distribution in the space. First, the temperature change

per inch in the vertical direction was examined for each of the sensor strands in order to identify the possible location of the neutral height. As is noted by Mateus & da Graça (2015), the greatest temperature change happens in the occupied zone. Above the neutral height, the temperature gradient goes to zero, meaning that this zone is well mixed, and the temperature of the air is consistent throughout (Mateus & da Graça, 2015). This is also where the highest temperatures can be found (Mateus & da Graça, 2015). Following this logic, it should be possible to locate the neutral height by finding the highest temperature reading vertically, above which the temperature change per inch is close to zero. To examine the temperature change per inch, the period of each cycling of the heater from on to off was examined. For each period, the maximum temperature, minimum temperature, and average temperatures were found. Then the average of these three temperatures for each period over the entire run for each treatment was found. In this way, the temperature gradient at the highest temperatures, lowest temperatures, and the average temperatures could be examined. These values were then used in the second method for examining the temperature gradients that follows.

The second method used for examining the temperature distribution in the space was detailed by Mateus and da Graça (2015), where non-dimensional variables are used to compare temperature profiles between experiments in which the room geometry varies between each experiment. The method is based on equation (22):

$$\theta = \frac{T - T_{in}}{T_{out} - T_{in}}, z = \frac{z}{z_{total}} \tag{22}$$

Where:

θ is temperature

Z is height

This method shows the temperature gradient over the height of the space, allowing the reader to see the location of the neutral height in the space, above which the temperature

gradient is much lower than in the rest of the space. As was noted above, the temperature gradient at the average maximum temperature, average minimum temperature, and overall average temperature are examined. The temperature gradients examined can be seen in the results section Figures 10-23. For the *Tin* value, the temperature of the air entering the space in the bottom hole in the blower door is used. The values used for *Tout* differ from those that are used in other experiments examined in this research.

The experiments conducted on DV systems are done during the cooling season, as the primary design for DV systems is for building ventilation and cooling (Mateus & da Graça, 2015). As such, the exhaust temperatures are the highest temperatures recorded in each experiment, as the exhaust is removing unwanted hot air from the space (Mateus & da Graça, 2015). In this experiment however, the highest temperatures are seen near the ceiling level in the space, and the exhaust is located below this level at the door. So as the air is pulled from the upper warm layer in the room, it cools down as it moves toward the exhaust located in the door, most likely due to heat loss across the door itself. For this reason, the *Tout* values that are used here are the highest temperatures that are seen on each strand close to the ceiling. Otherwise the use of the exhaust temperature in the space would give a false depiction of the temperature gradient for each sensor strand.

Research Questions 2 & 3 Data Analysis Procedure

The original intent of this portion of the experiment was to use the inputs that were present in the experimental phase as a basis for developing the energy model, and to then find a way to compare the three temperature outputs (*Tfloor, Toccupied, and Tmixed*) to the temperatures that were recorded in the experiment. Given the high number of sensors that were used in this experiment, it was necessary to find a way to average all of the temperatures in the building such that three temperatures could be produced that were representative of the three different subzones in the building. A method of averaging all of the temperatures

according to the zones in the model would be devised, with the location of the neutral height in the test building being assigned according to the predicted location of the neutral height from the model. As will be discussed in the results section of this paper, the neutral height predicted by the model was not as expected, due to unforeseen errors in the results of the modeling portion of this experiment. The original method of averaging the temperatures in the test building, such that three temperatures can be examined (*Tfloor, Toccupied, and Tmixed*), was carried out, regardless of the discrepancies between expected results from the model, and actual results from the model. To do this, a volumetric weighting method was devised.

A three-dimensional model was used, identical to what was used in the OpenStudio® model of the test building. Graphical representations of the location of the sensors in the test building were placed in the model. A three-dimensional box or volume was placed around each sensor. The size and location of the volume around each sensor was meant to coincide with the temperature readings at each sensor, and how much of the air in the test building could be assumed to be at the same temperature as the air at each sensor, according to variables that would affect temperature readings in the test building. In other words, a volume corresponding to the surrounding conditions that were assumed to be representative of the same conditions at the exact location of each sensor was created around the space in which each sensor was located. This means that the sensors located closest to the walls and ceilings were representative of a smaller volume of the overall space of the test building, due to their close proximity to surfaces that were potentially cooler than the air in the space, which may have affected the temperature readings for these sensors.

The sensors located on the medium strand were closest to the middle of the space, and furthest from any factors in the space that would affect the temperature readings at these locations, and as such these sensors were given the largest weight in the space. Each volume was then assigned its weighting factor according to the proportion of the given volume in

relation to the entire volume of the interior space in the test building. This weighting factor was then used to average the temperature readings from the sensors in the test building. A graphic of the volumetric weighting method can be seen in Figure 9. Each three-dimensional box seen in the image corresponds to the location of a sensor on a strand. The significance of the colors of each volume are as follows: red represents the mixed zone, orange represents the occupied zone, and blue represents the floor zone.

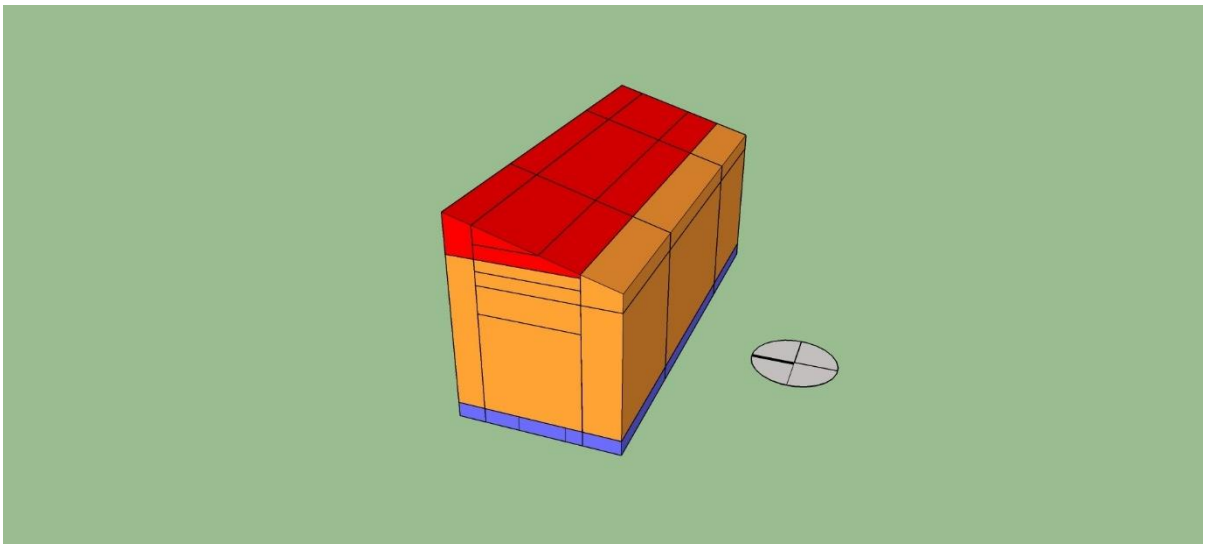

Figure 9. Three-dimensional volumetric weighting method.

CHAPTER 4: RESULTS

The following results are from four different experimental runs. The runs were chosen according to which sets of data were most representative of the typical results and experimental conditions that were seen during this experiment. Two runs for which results will be shown are 15 ACH@50. The other two runs for which results will be shown are a baseline run (no air-flow), and a run with 5 ACH@50.

Research Question 1 Results

As was noted earlier in this paper, the first question that was addressed was: Is there thermal stratification in buildings with loosely constructed envelopes and no centralized forced air system in the heating season? The answer is yes. As one might expect, there is thermal stratification in buildings under the aforementioned conditions. However, whether the stratification is non-linear, or linear, remains unclear due to circumstances which will be discussed later in this paper.

The following figures show the temperature gradients over three different treatments used in three different runs; one treatment with no airflow (baseline), one treatment with 5 ACH@50, and one treatment with 15 ACH@50. The temperature gradients examined are those that were previously mentioned in the methods section of this paper, averaged from each cycle of the heater from on to off; the temperature gradient at the average maximum temperature recorded, the average minimum temperature recorded, and the overall average temperature recorded. Again, the method used for this approach is the same noted by Mateus and da Graça (2015), which uses equation (22):

$$\theta = \frac{T - T_{in}}{T_{out} - T_{in}}, z = \frac{z}{z_{total}} \tag{22}$$

The temperature gradients shown in Figures 10-23 show the temperature gradients at the three different sensor strands with the highest resolution; M1, M2, and M3. Also displayed with the temperature gradients are Tables 1-3, which show the temperatures used in equation (22), and the corresponding average temperature change per inch. It should be noted that the inlet temperature was included in these tables, but does not have an associated height in the table. The temperature sensor that recorded the inlet temperature was located in the center of the bottom opening in the custom blower door that was made for the purposes of this experiment. The height of this temperature sensor is approximately 8", but this height is not taken into account in the change per inch in any way. The inlet temperature is recording the temperature of the air entering the space through the duct blaster from the exterior of the building.

Table 1 *Temperature 1M Average Maximum*

1M Avg Max 15 ACH@50		
H (in)	Temp°C	ΔT/inch
Inlet	12.41048	N/A
4	17.02394	N/A
48	21.48583	0.10141
72	22.98578	0.06250
78	22.94417	-0.00694
84	23.10383	0.02661
90	23.87833	0.12908
96	23.76728	-0.01851

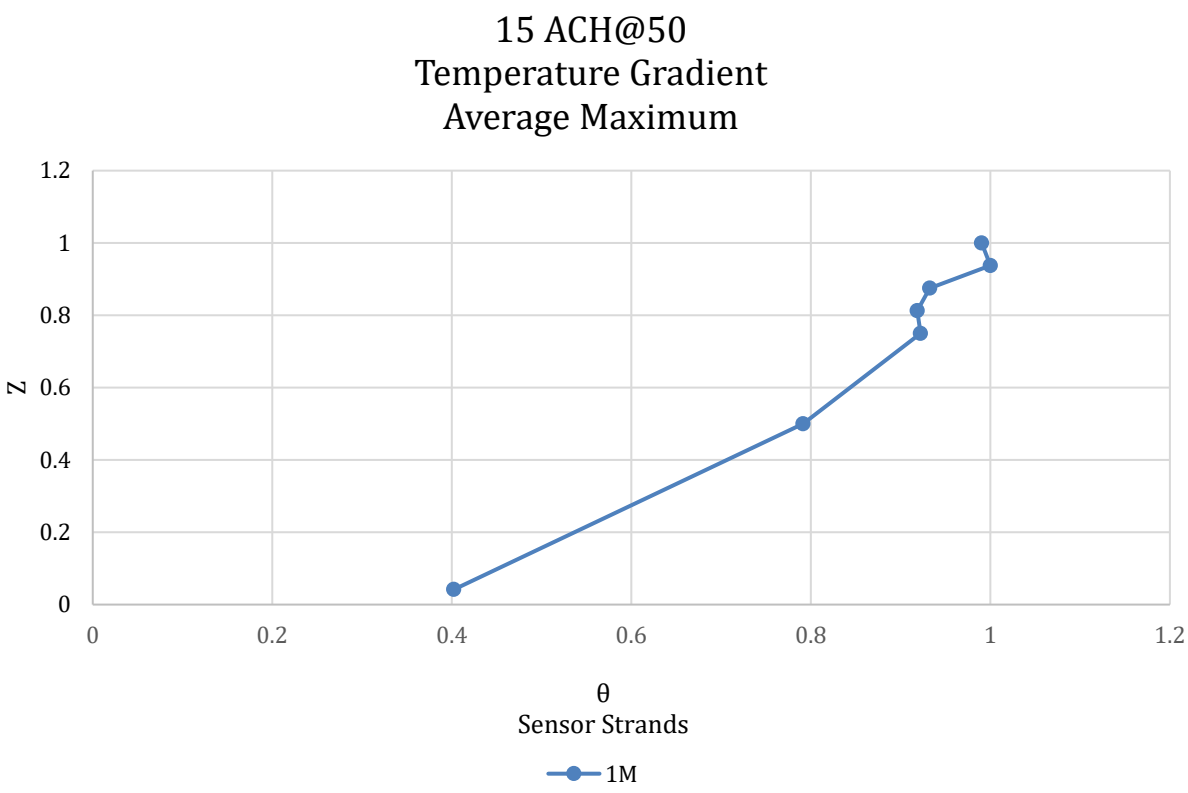

Figure 10. 15 ACH@50 Temperature gradient average maximum strand 1M.

Table 2 *Temperature 2M Average Maximum*

2M Avg Max 15 ACH@50		
H (in)	Temp℃	ΔT/inch
Inlet	12.41048	N/A
4	17.88172	N/A
48	21.66983	0.08609
72	23.12478	0.06062
78	23.33650	0.03529
84	23.72194	0.06424
90	24.51011	0.13136
96	24.28789	-0.03704

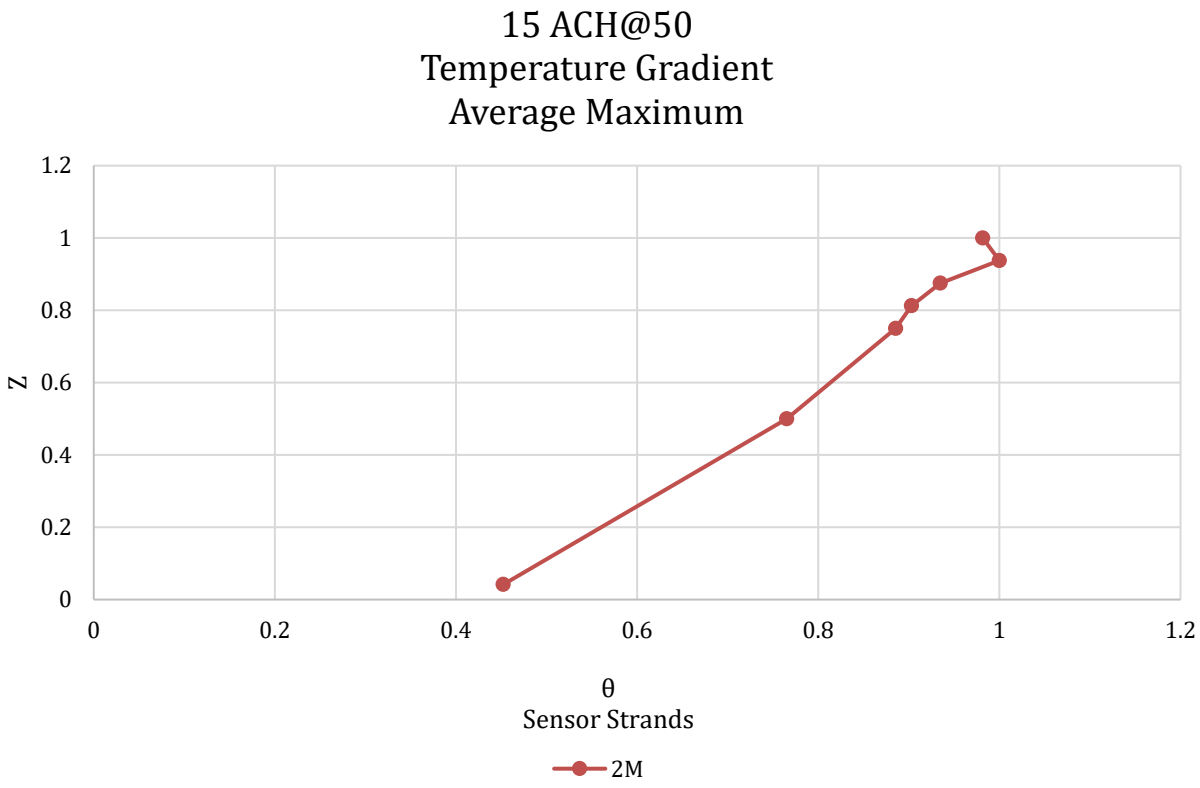

Figure 11. 15 ACH@50 Temperature gradient average maximum strand 2M.

Table 3 *Temperature 3M Average Maximum*

3M Avg Max 15 ACH@50		
H (in)	Temp°C	ΔT/inch
Inlet	12.41048	N/A
4	19.02061	N/A
48	21.95461	0.06668
72	24.27061	0.09650
78	24.73939	0.07813
84	24.67333	-0.01101
90	25.10050	0.07119
96	25.48933	0.06481

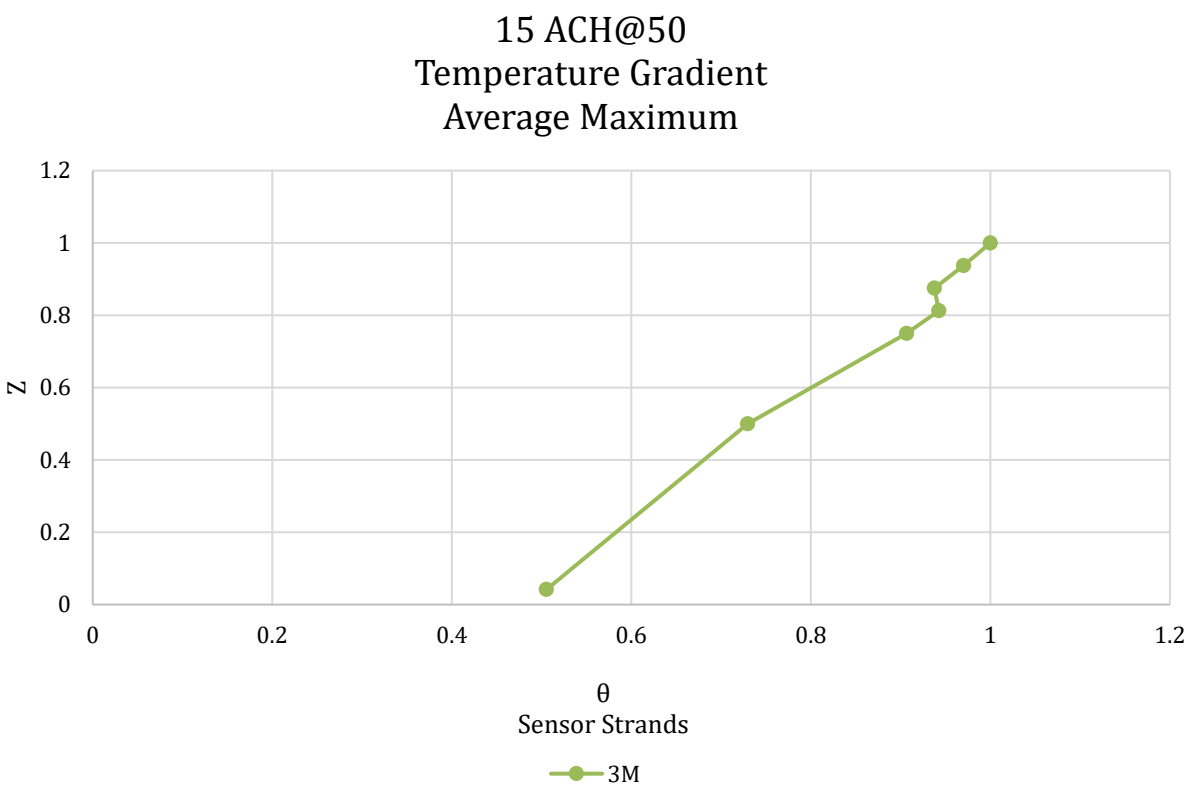

Figure 12. 15 ACH@50 Temperature gradient average maximum strand 3M.

Temperature nodes two and three are located at 90" and 84" respectively. It is this area, in between nodes two and three, that the neutral height location was predicted. As can be seen in Table 2, the temperature change between these two nodes is an order of magnitude greater per inch than in the rest of the space. While this is also true for table 1, the change per inch is not as consistent due to the close proximity of sensor strand 1M to the door where cold air is coming in. Sensor strand 3M also deviates from this pattern, due to its close proximity to the heater. In light of this it was assumed that this larger temperature change per inch indicates a transition from the occupied zone to the mixed zone, where the air is at the highest temperatures present in the space.

The temperature gradient in some places in the upper region of the space appears as though it is going to transition to zero or near zero, as it does when the transition between the occupied zone to the well mixed zone occurs, but then the gradient increases again. This may suggest that if there is a neutral height located where it was predicted, that the mixed zone is much smaller than what was expected, and due to the resolution of the sensors on the strands, the mixed zone is not apparent. It may also be that the space in the test building is stratified, but has a linear temperature profile. This notion will be discussed in the next section of results. The temperature gradient is fairly consistent among the three different medium length sensor strands at the average maximum, as well as the overall average temperatures that are seen. These profiles are also consistent under different testing treatments. The gradient at the average minimum temperatures varies, however, as the temperatures throughout the space have a narrower range, being at the coldest point before the heater switches back to the on position. The aforementioned gradients are as depicted in Figures 13-21.

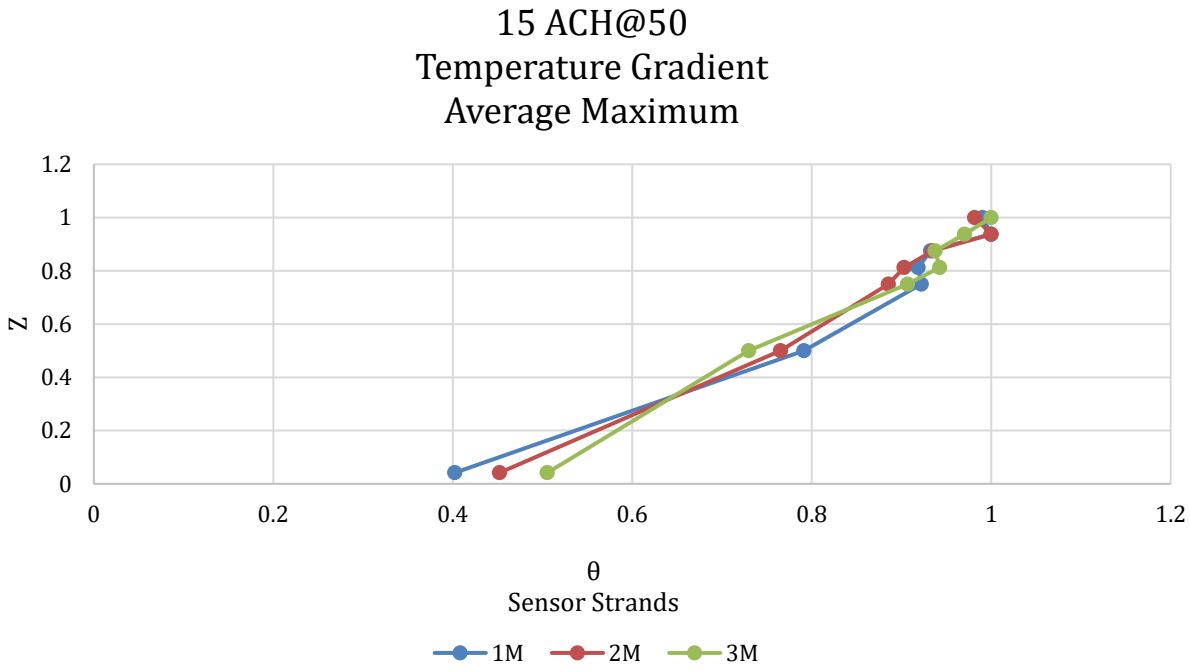

Figure 13. 15 ACH@50 Temperature gradient average maximum.

Table 4 *Medium Strand Temperatures Average Minimum*

Average Minimum Temperatures 15 ACH@50		
1M Min Temp	2M Min Temp	3M Min Temp
16.4512	17.3296	18.0449
19.5206	19.5483	19.7289
19.8468	19.8398	20.2672
19.6492	20.0173	20.4753
19.7079	19.9442	20.4407
20.0414	20.2116	20.4893
19.8678	20.1316	20.2776

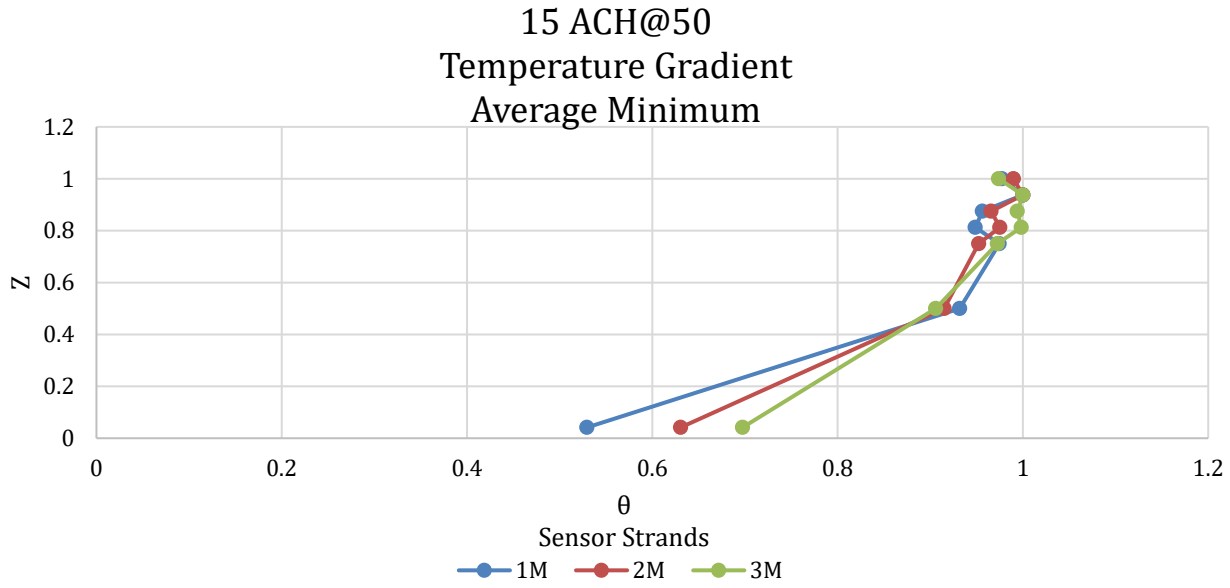

Figure 14. 15 ACH@50 temperature gradient average minimum.

Table 5 *Medium Strand Temperatures Overall Average*

Overall Average Temperatures 15 ACH@50

1M Avg Temp	2M Avg Temp	3M Avg Temp
16.7318	17.6042	18.5068
20.4353	20.5377	20.7770
21.2903	21.3506	22.0832
21.1523	21.5315	22.3969
21.2518	21.6695	22.3285
21.7889	22.1473	22.5328
21.6305	22.0031	22.5779

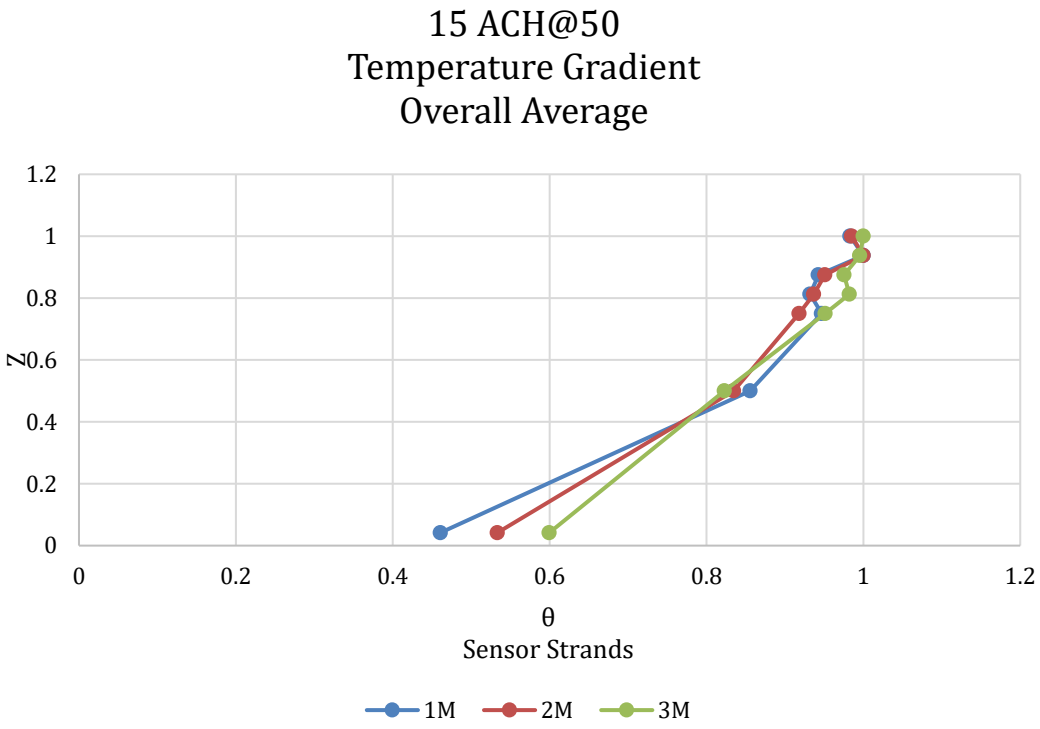

Figure 15. 15 ACH@50 Temperature gradient overall average.

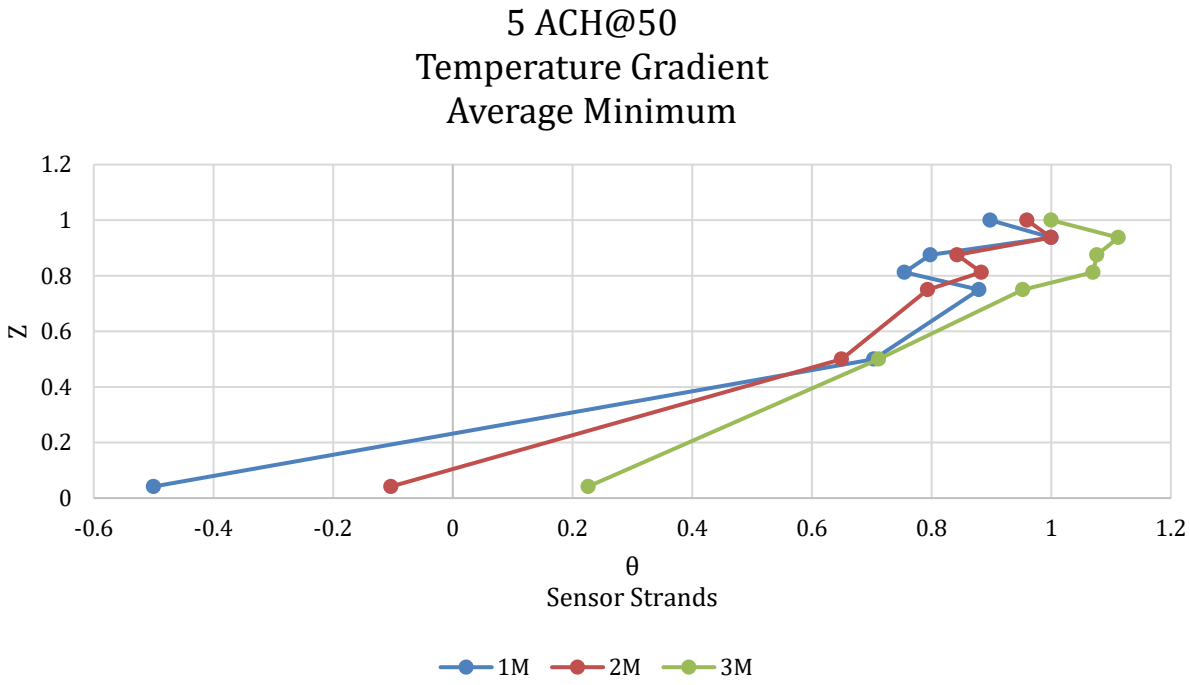

Figure 16. 5 ACH@50 Temperature gradient average minimum.

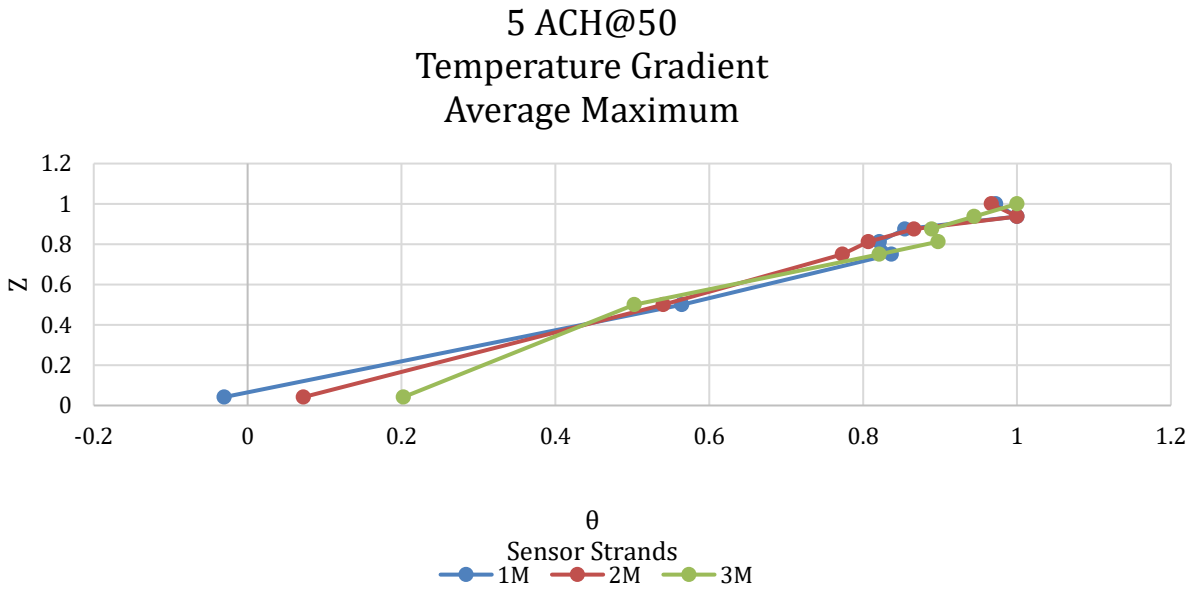

Figure 17. 5 ACH@50 Temperature gradient average maximum.

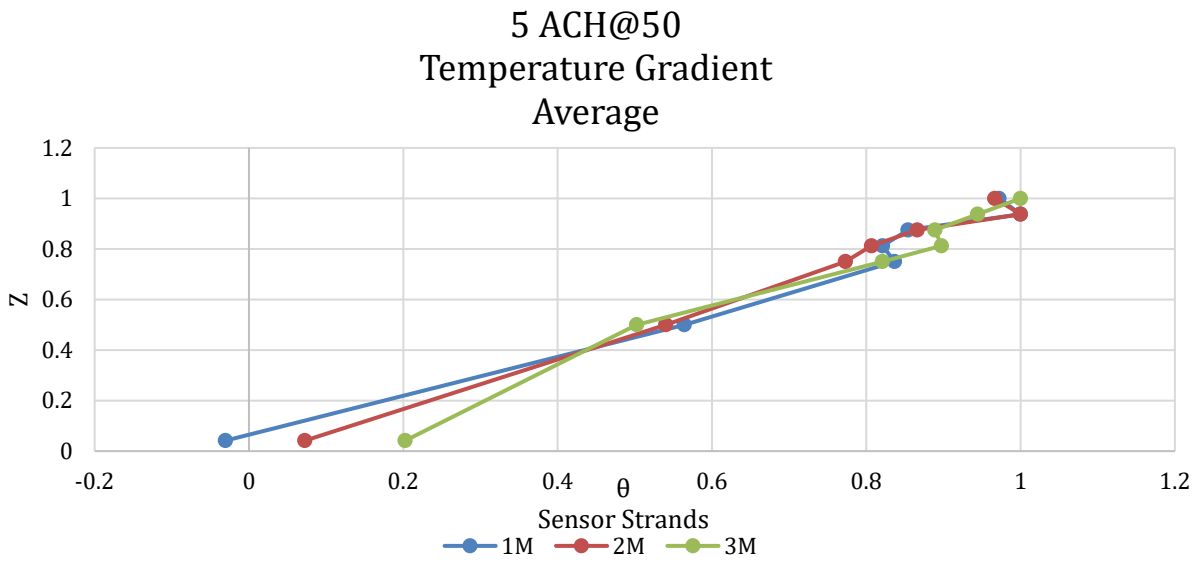

Figure 18. 5 ACH@50 Temperature gradient overall average.

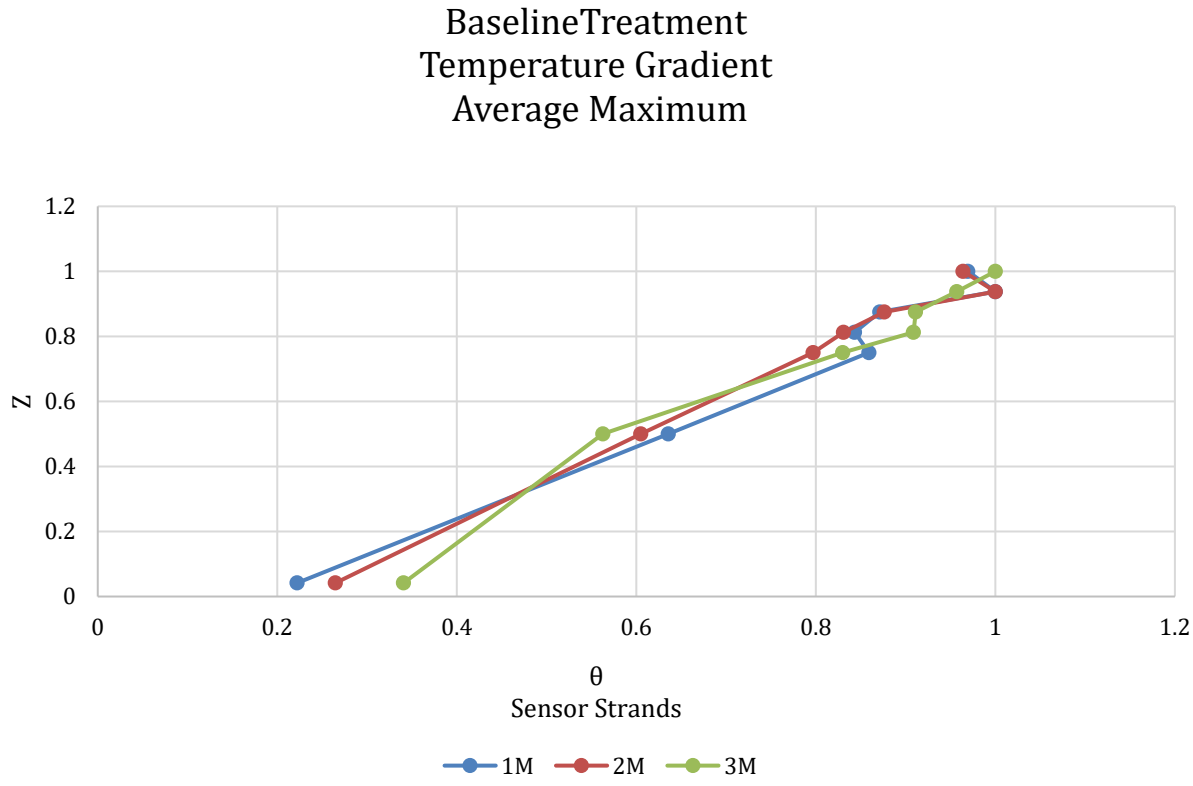

Figure 19. 5 ACH@50 Temperature gradient average maximum.

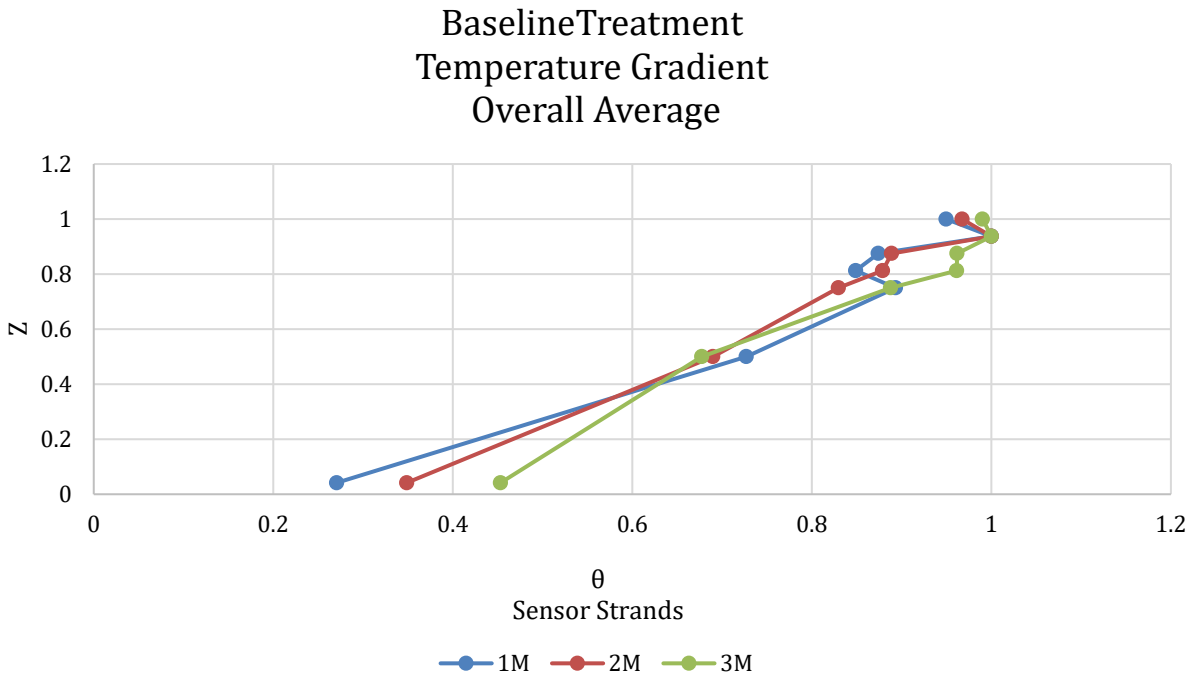

Figure 20. Baseline temperature gradient overall average.

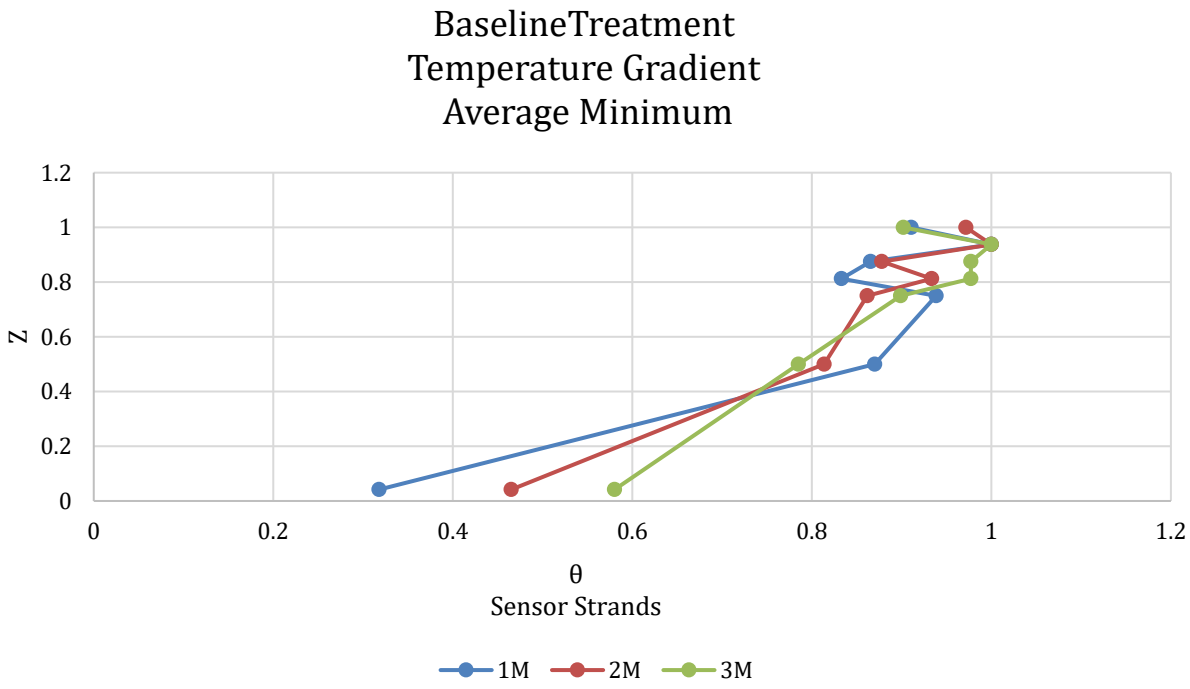

Figure 21. Baseline temperature gradient average minimum.

To further verify that the temperature gradient in the test building is present in varying conditions, the graph shown in Figure 22 depicts a comparison between the temperature gradient at the coldest exterior temperature that was experienced during the run, and the warmest exterior temperature during the run.

Table 6 *Temperatures Used in the Gradients Shown in Figure 22*

Warm, Cold		
Height (in)	Warm ℃	Cold ℃
Exterior	18.437 ℃	1.3 ℃
Inlet	18.437	16.437
4	17.875	17.625
48	21.500	20.875
72	23.062	22.312
78	23.187	22.562
84	23.687	23.000
90	24.500	23.812
96	24.250	23.562

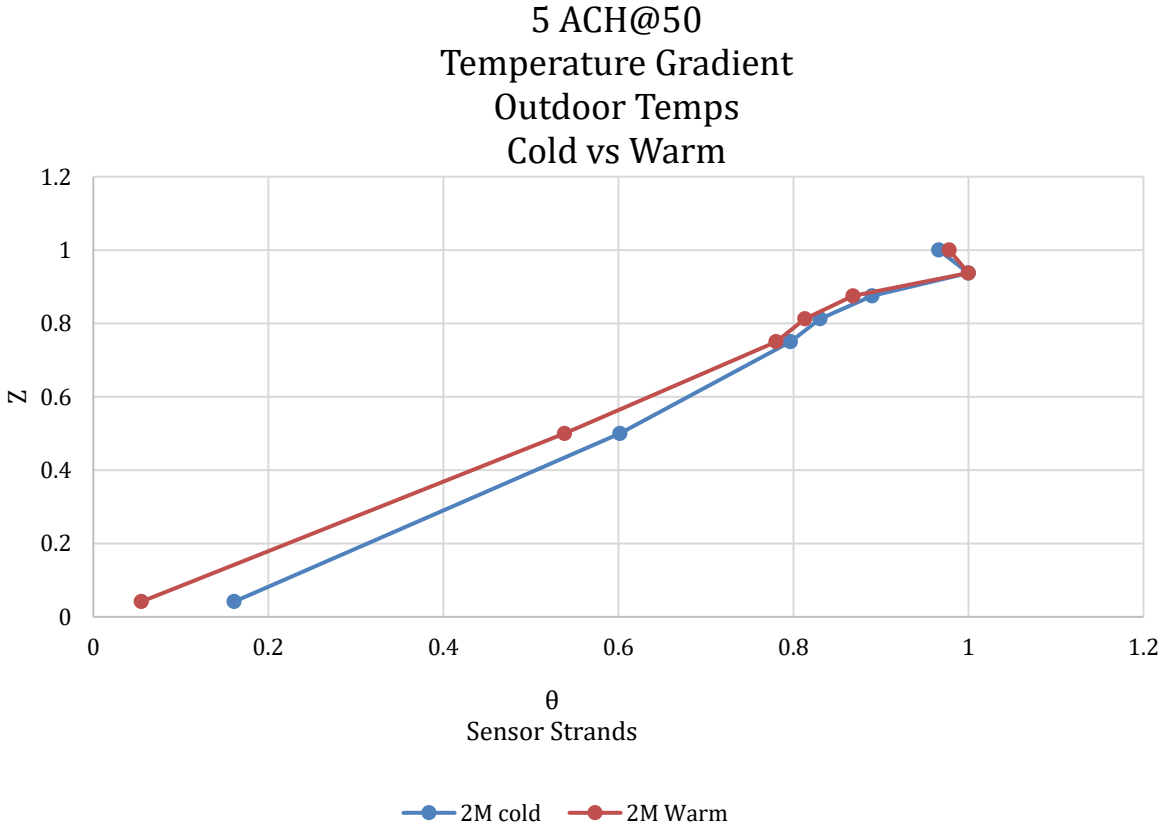

Figure 22. 5 ACH@50 Temperature gradient outdoor temperatures cold vs warm.

The final graph shown depicts the temperature gradient for the average maximum temperatures on sensor strand M2 between each of the different experimental treatments. It can be seen that the gradient curve is consistent among all three treatments.

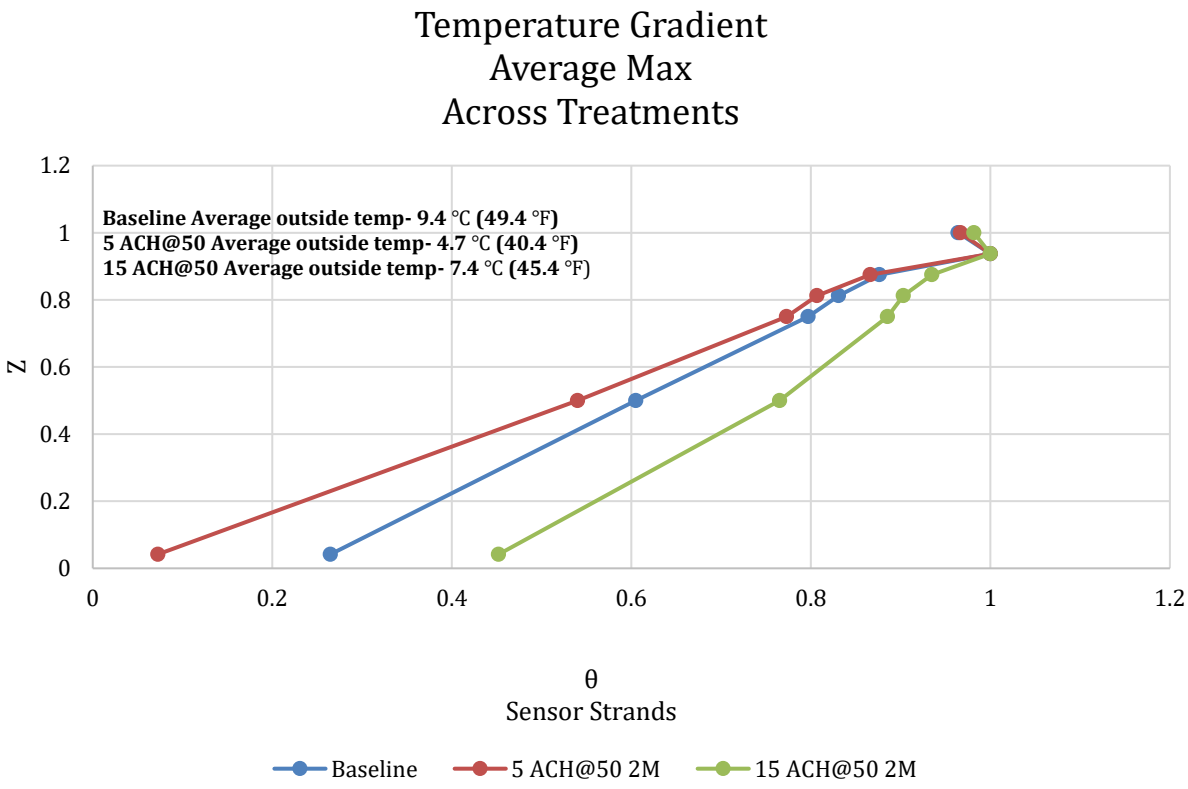

Figure 23.Temperature gradient average maximum across treatments.

Research Question 2 Results

As was stated in the methodology section of this paper, the initial intent was to model the test building using the parameters that were present during the experimental portion of this research, and use the predicted neutral height from the model to develop a weighted method of averaging the temperature data from the test building in order to produce three different temperatures that match those that are the outputs from the model; *Tfloor, Toccupied, Tmixed*. Unfortunately, the results of the model were not as expected. The treatment that was used in the experiment with the highest air flow rate was 15 ACH@50. This equates to approximately .75 ACHn. With this airflow rate used in the model, the iterative solver in the model did not show the interior temperatures to be stratified, and as such the results produced

by the model showed a well-mixed temperature profile. It was not until the airflow used was approximately 30 ACH@50 (2ACHn), that the model showed stratification in the outputs. This

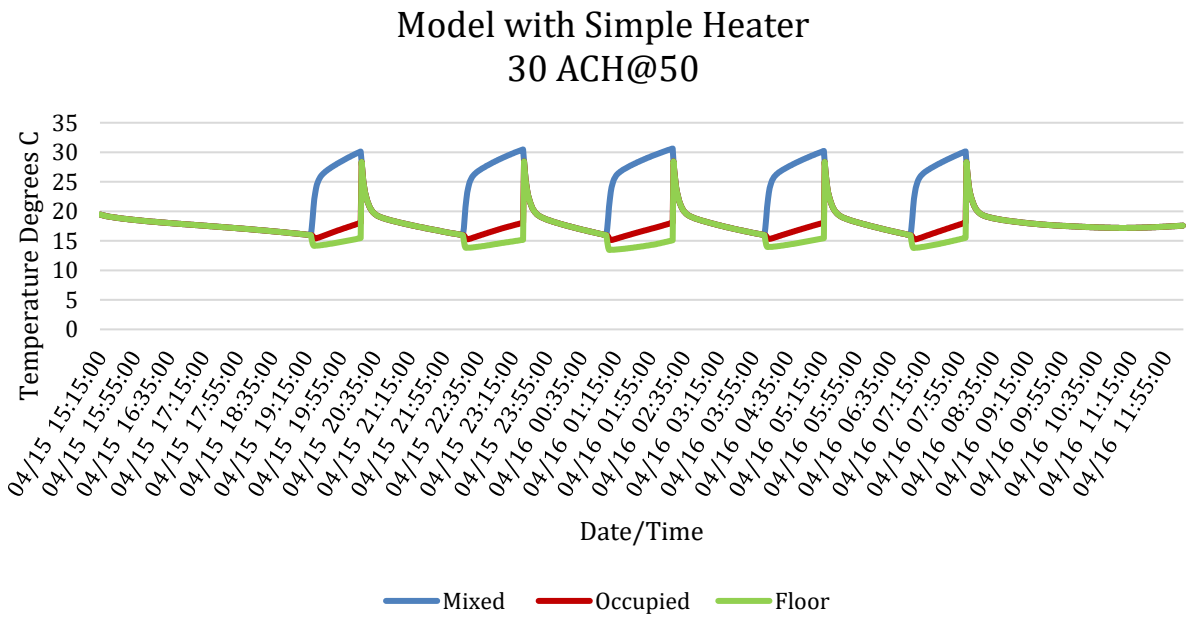

Figure 24. Stratified model output using simple heater configuration.

airflow value is not one which was used in any of the testing treatments for airflow in the test building experimental runs. Figure 24 shows the model switching back and forth between well mixed and stratified at the higher airflow rate of 30 ACH@50.

When the heater cycles on and off, the iterative solver in EnergyPlus™ cycles between performing calculations for a thermally stratified model and a well-mixed model. This can be seen in the temperature profile in Figure 24 where all of the temperatures from the different subzones converge back into one single temperature reading. This can be accounted for in the equation for the prediction of the height of the boundary layer Fr_{hb} in the models (U.S. Department of Energy, 2018a):

$$Fr_{hb} = \left(\frac{24.55}{H_{ceil}}\right)\left(\frac{0.000833 \times MCP_{tot}}{N_{plumes} \times \dot{Q}_{perplume}^{\frac{1}{3}}}\right)^{\frac{3}{5}} \quad (23)$$

In typical scenarios where a DV system is used for space conditioning, there are multiple internal gains such as computers, office equipment, task lights, people, etc. As was noted earlier, the value for $\dot{Q}$ in the EnergyPlus™ Three-Node DV model incorporates all of those internal gains. Due to an oversight in the setup, the only internal gain in the experimental setup in the test building was the radiant heater. When the heater in the model cycles on and off, the value of $\dot{Q}$ goes from approximately 1500 W, to 0 W. When this happens, the model goes from a thermally stratified configuration, to a well-mixed configuration, due to the fact that when trying to predict the height of the boundary layer the program is trying to divide by zero.

In reality, when the heater thermostat is calling for heating, the electrical resistance elements in the heater are inputting heat energy into the oil in the heater, where it is stored. When the thermostat on the heater is satisfied, the flow of current that is being supplied to the heating elements is interrupted. However, a portion of the energy that was input into the oil in the heater is still present and being slowly released into the space. So, even though the heater is not constantly in heating mode, there is almost always a varying flow of heat energy into the space. For this reason, a customized baseboard heater with a more realistic heating curve was created using the EnergyPlus™ EMS, to examine whether the resultant output from the model would more closely represent the measured data. The heater input into the model was manipulated such that once the heater turns on and begins heating the zone, the power input from the heater is a fraction of the total power (1500 W), depending on the amount of time the thermostat has been calling for heat. As the room heats up, the heating power input begins at a

smaller fraction, and increases to full power over a given length of time. Once the heater reaches full power and the setpoint is reached, the heater power input is reduced incrementally over a period of time. This is representative of the curve of heat energy that is input into the zone from the actual heater. Unfortunately, while the heating curve produced by the radiant heater in the model more closely represents what is happening in the test building, it is still necessary to set the airflow rate to an unrealistically high input for the zone to be thermally stratified. The temperature profile from the customized heater model can be seen in Figure 25 with the infiltration rate 30 ACH@50.

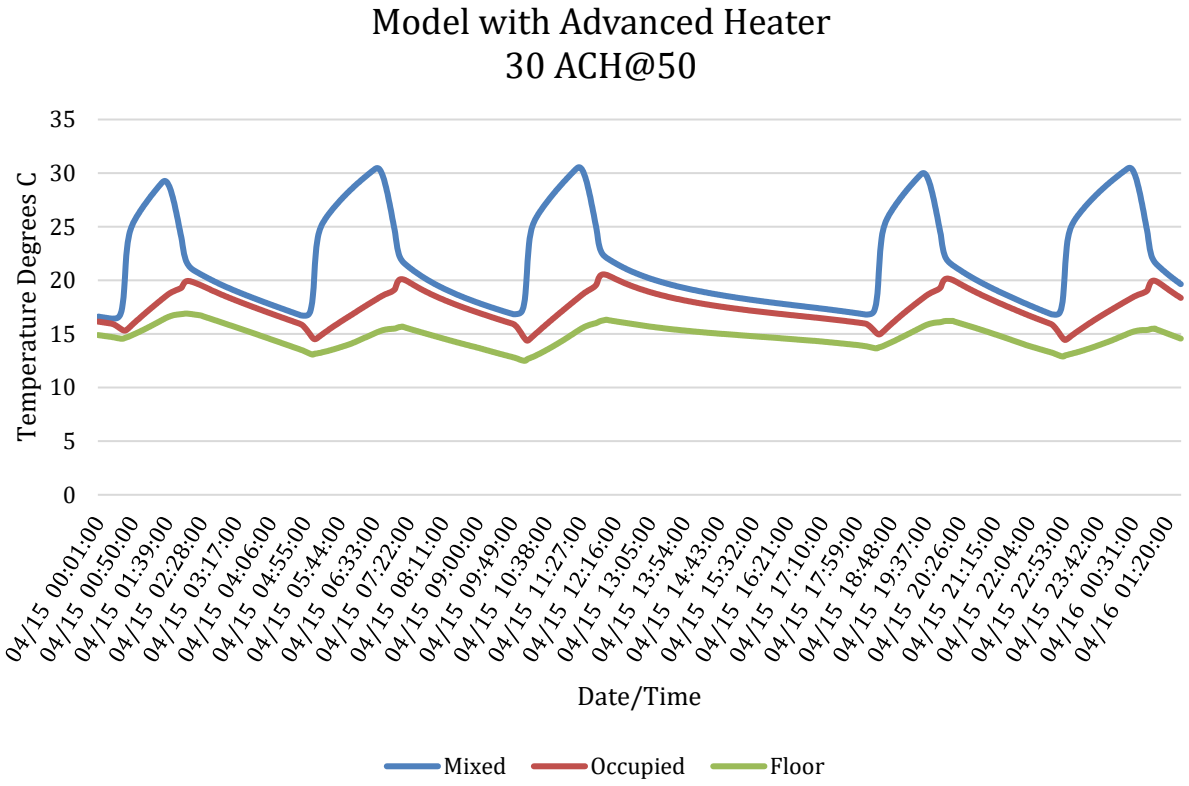

Figure 25. Temperature Profile from customized heater input.

Even with the heating curve being more closely in line with a real heating curve from this type of appliance, the model still predicted transition heights that differed greatly from what was expected, and often reported an error value of -9.99 meters as the transition height

(neutral height). As was stated previously in the review of literature, the conditions under which the model will revert to well mixed (or in this case report an error value) are as follows:

- Whenever $Tmixed<Toccupied$
- Whenever $MCPtotal \leq 0$
- Whenever $Hfr * Hceil < Hfl,top + \Delta zocc,min$

It is the last condition that caused the model to report an error value. Whenever the height fraction (*Hfr*) multiplied by the height of the ceiling (*Hceil*), the product of which is the predicted neutral height, is less than the minimum height of the floor zone plus the minimum change in height of the occupied zone, both of which are .2 meters (0.065 ft), the model will give an error value of -9.99 meters for the transition height.

Even though the model is not producing results that were the same as those predicted in this research, it is the opinion of the author that further research needs to be done on modeling thermally stratified buildings during the heating season. One of the average temperature ranges for an experimental run in the test building can be seen in Table 7. Figure 26 shows the test building and a representation of the size of the heater used in this experiment in relation to the size of the test building space.

Table 7 *Temperature 2M Average Max*

2M Avg Max 15 ACH@50

H (in)	Temp°C	ΔT/inch
4	17.88172	N/A
24	19.60352	N/A
48	21.66983	0.08609
72	23.12478	0.06062
78	23.3365	0.03529
84	23.72194	0.06424
90	24.51011	0.13136
96	24.28789	-0.03704
Average	22.64754	N/A

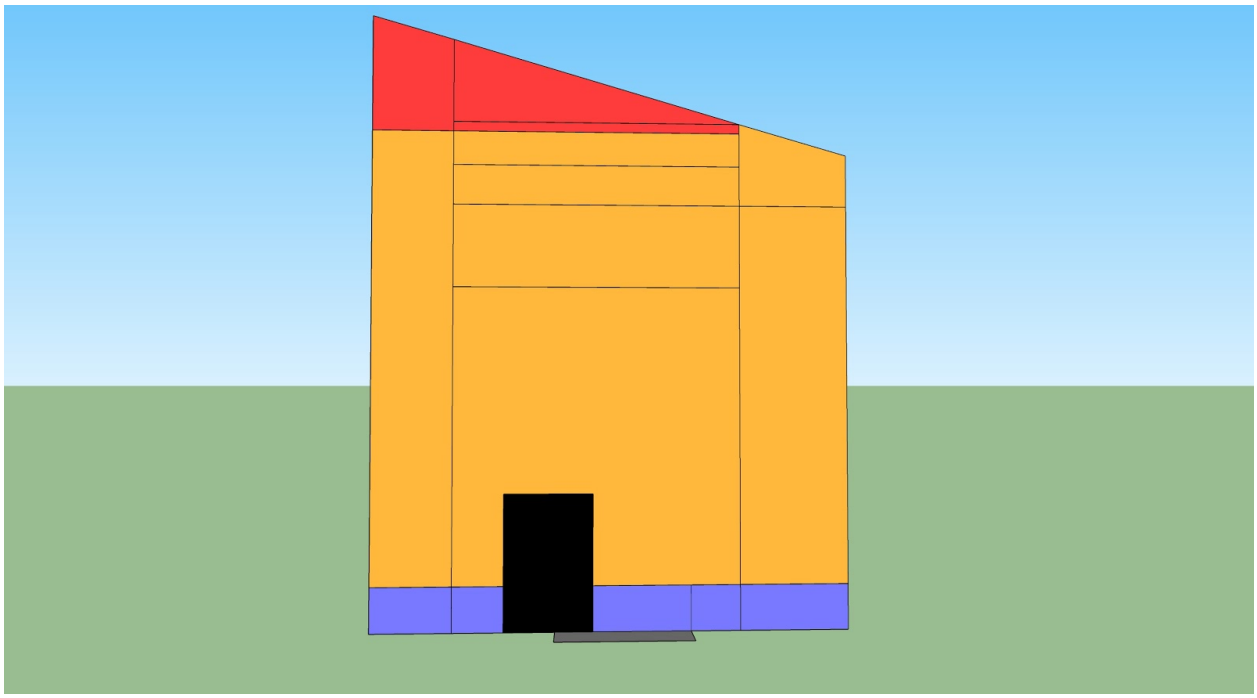

Figure 26. Building elevation with radiant heater.

The thermostat on the heater is located at less than the height of the top of the heater, which is approximately 24". For the discussion that follows, we will assume that the height of the top of the heater will coincide with the thermostat height for the purpose of simplifying assumptions. The placement of the sensors vertically on the strands is such that there is no way to know exactly what the temperature is at the height that coincides with the top of the heater. If the known temperatures at two known heights are used, 4" and 48", the temperature change per inch can be used to find an approximate assumed temperature at the height of the top of the heater, 24". When this is done, and an assumed temperature is produced at 24", it can be seen that the assumed temperature at this height is approximately 3˚C less than the average of all of the known temperatures.

If the assumptions made here are reasonably accurate, it can be deduced that in a well-mixed model that uses the average of temperatures in a zone to determine the zone HVAC equipment operation mode, the heater will run less than the heater in a model that is representative of a space that in reality is thermally stratified. Theoretically this will result in a false depiction of heater energy use from the well-mixed model, with this model showing less energy used than a thermally stratified model, as the well mixed model uses the average temperature in a zone which is warmer than the temperatures that are experienced in reality at the thermostat height for the heater. Figures 27-30 show the temperature profiles from the data gathered in this experiment when compared with both a well-mixed model, and the results of the thermally stratified model. It should again be noted here that the thermally stratified model uses an air change rate that is higher than what was actually used in the experimental procedures in this research.

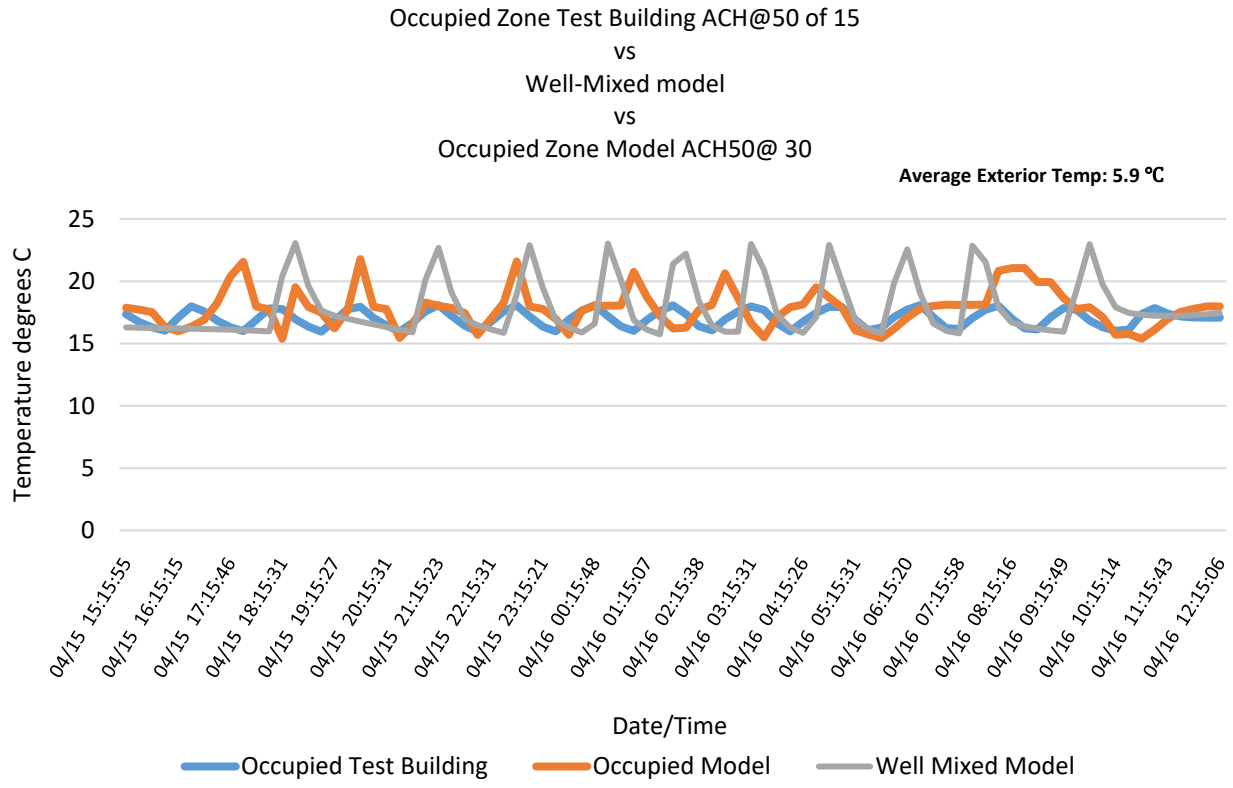

Figure 27. Occupied zone test building vs well mixed model vs occupied model.

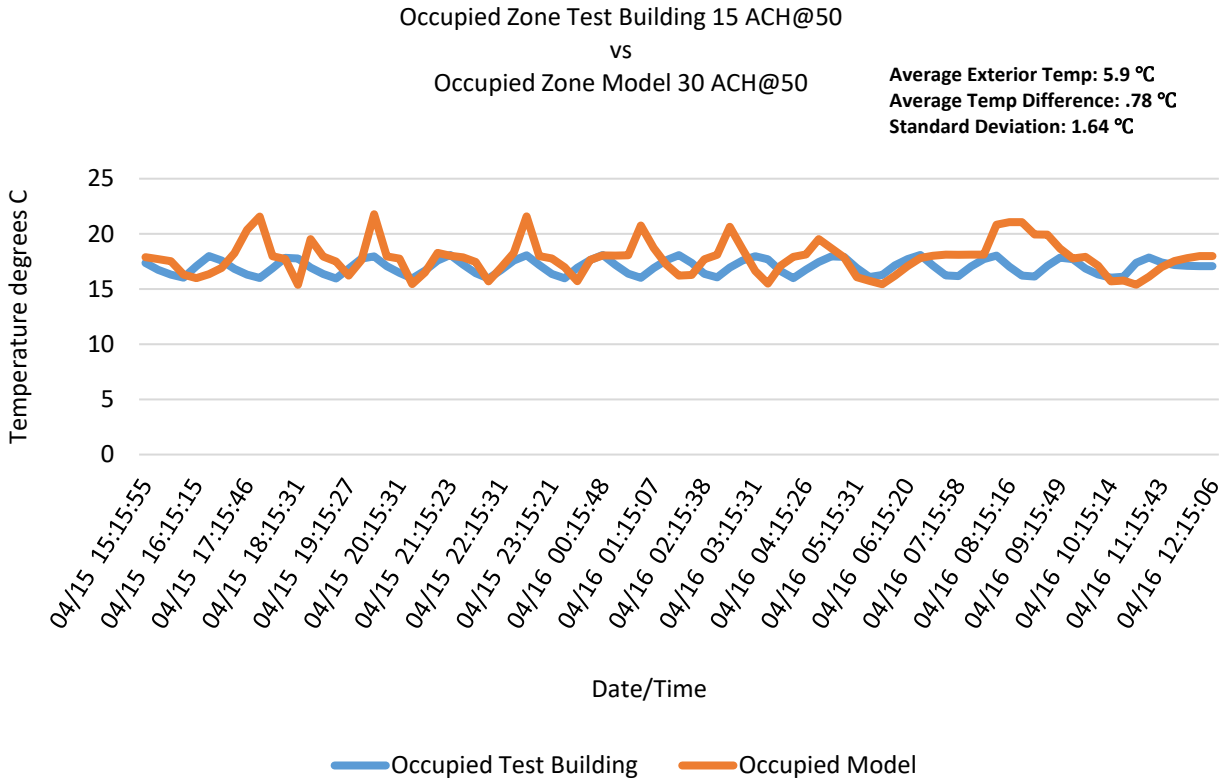

Figure 28. Occupied zone test building vs occupied zone model.

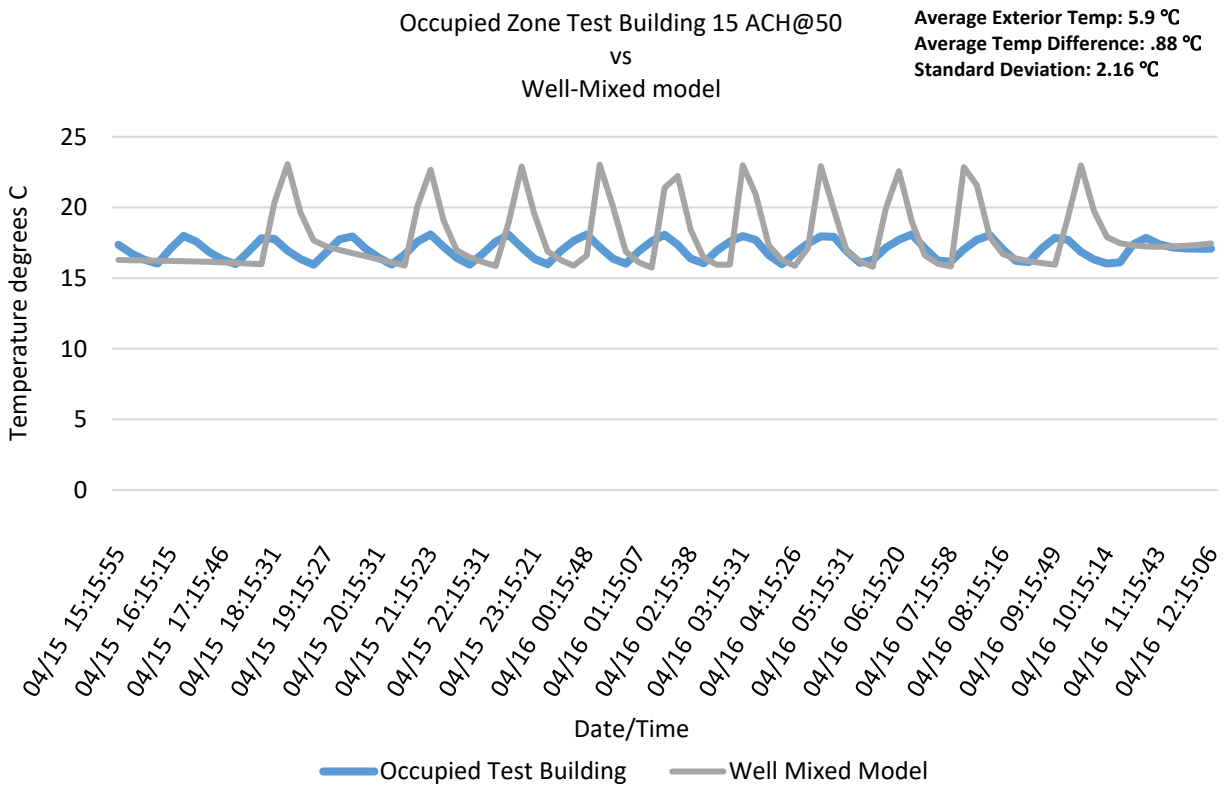

Figure 29. Occupied zone test building vs well-mixed model.

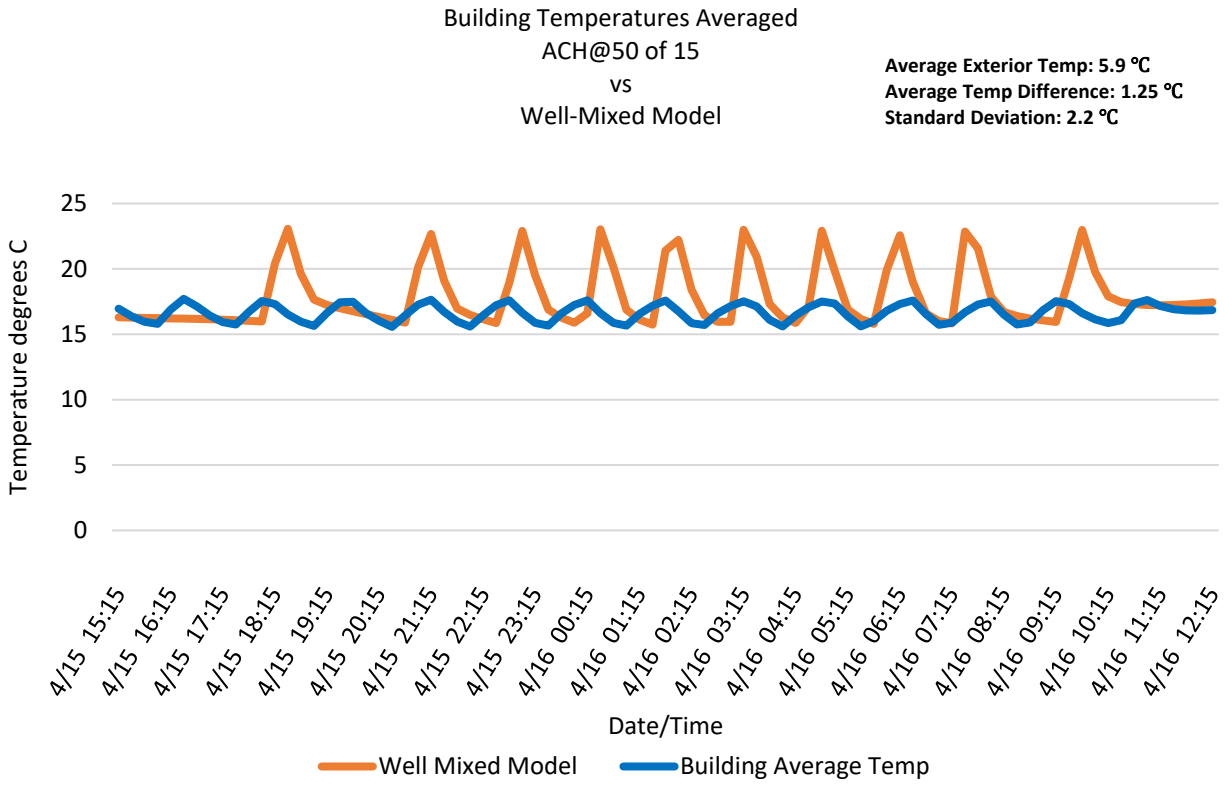

Figure 30. Well-mixed building temperature average vs well-mixed model.

It can be seen that the well mixed model shows maximum temperatures that are much higher than those recorded in the occupied zone of the test building, as well as the averaged temperatures of the test building. This supports the assumption that the heater in a model that assumes well mixed air, and averages the temperatures, will run more than a model that is representative of a thermally stratified building when modeling buildings that are subject to high levels of infiltration during the heating season.

Research Question 2 & 3 Results

As was stated by da Graça (2003), in the design of DV systems the ratio between the heat gain $\dot{Q}$ and airflow MCP_{tot} is the most important parameter for assuring the effective

operation of the DV system, and the value of this ratio has a very small range in which it should be set in order to achieve ideal operating conditions for a given space. While using the EnergyPlus™ Three-Node Displacement Ventilation RoomAir Model may not be the most appropriate approach for modeling buildings constructed with low levels of air sealing and insulation, this research has provided some insight into further steps that can be taken in the quest for finding a more suitable approach to modeling the conditions in question. The data in the results from question 1 were initially interpreted as there being a neutral height between 84" and 90". However, given the conditions set forth in this experiment, this could not be fully validated. The model results show that at higher air-flow rates, there is a neutral height, but it is located considerably lower than what was predicted in this research. This also cannot be validated, due to the low resolution in the sensor strands in the lower regions of the space. In order to gain a better understanding of where the model predicted neutral height lies based on the ratio of $\dot{Q}$ and MCP_{tot} in equation 14, three tables were generated using the equation for the prediction of the height boundary layer Fr_{hb} (the neutral height), for three different building volumes. These tables show how varying the ratio between $\dot{Q}$, represented here as Power in watts, and MCP_{tot} affects the outcome of the model predicted height of the boundary layer Fr_{hb}.

$$Fr_{hb} = \left(\frac{24.55}{H_{ceil}}\right)\left(\frac{0.000833 \times MCP_{tot}}{N_{plumes} \times \dot{Q}_{perplume}^{\frac{1}{3}}}\right)^{\frac{3}{5}} \tag{14}$$

Table 8 shows the color-coding scheme used in the tables for the model predicted neutral height location. Here again it should be noted that whenever the height fraction (*Hfr*) multiplied by the height of the ceiling (*Hceil*), the product of which is the predicted neutral height, is less than the minimum height of the floor zone plus the minimum required change in height of the occupied zone, the total of which is .4 meters (0.13 ft), the model will give an error

value of -9.99 meters for the neutral height. The first two tables produced are using building volumes of 1280 ft^3 and 2119 ft^3, which coincide with the size of the test building used in this research and the size of a building from the South Africa research by Ramsdell et al. (2105) respectively. The last building volume of 4238 ft^3 was used for the purposes of showing the same inputs for heat gain with a higher airflow.

.

Table 8 *Color-coding scheme for model predicted neutral heights*

Color Scale for Neutral Height Location	Feet
Model Failure	<1.3
Lower Occupied Space	1.3 - 4
Upper Occupied	4 - 6
Mixed Space	6 - 15
Above 15'	> 15

Table 9 *Heat gain vs airflow for 1280 ft3*

ACHn	Predicted Neutral Height (ft) Volume-1280 ft^3											
5	8.32	7.24	6.38	5.56	4.84	4.46	4.21	4.03	3.88	3.77	3.67	3.51
4.5	7.81	6.80	5.99	5.22	4.54	4.19	3.95	3.78	3.65	3.54	3.44	3.29
4	7.27	6.33	5.58	4.86	4.23	3.90	3.68	3.52	3.40	3.29	3.21	3.07
3.5	6.71	5.84	5.15	4.49	3.91	3.60	3.40	3.25	3.14	3.04	2.96	2.83
3	6.12	5.33	4.70	4.09	3.56	3.28	3.10	2.96	2.86	2.77	2.70	2.58
2.5	5.49	4.78	4.21	3.67	3.19	2.94	2.78	2.66	2.56	2.48	2.42	2.31
2	4.80	4.18	3.68	3.21	2.79	2.57	2.43	2.32	2.24	2.17	2.12	2.02
1.5	4.04	3.52	3.10	2.70	2.35	2.17	2.05	1.96	1.89	1.83	1.78	1.70
1	3.17	2.76	2.43	2.12	1.84	1.70	1.60	1.53	1.48	1.43	1.40	1.34
0.5	2.09	1.82	1.60	1.40	1.22	1.12	1.06	1.01	0.98	0.95	0.92	0.88
0	**20**	**40**	**75**	**150**	**300**	**450**	**600**	**750**	**900**	**1050**	**1200**	**1500**
	Power W											

Table 10 *Heat gain vs airflow for 2119 ft3*

ACHn	Predicted Neutral Height (ft) Volume-2119 ft^3											
5	11.25	9.80	8.64	7.52	6.55	6.04	5.70	5.45	5.26	5.10	4.96	4.74
4.5	10.56	9.20	8.11	7.06	6.15	5.67	5.35	5.12	4.93	4.78	4.66	4.45
4	9.84	8.57	7.56	6.58	5.73	5.28	4.99	4.77	4.60	4.46	4.34	4.15
3.5	9.08	7.91	6.97	6.07	5.29	4.87	4.60	4.40	4.24	4.11	4.01	3.83
3	8.28	7.21	6.36	5.53	4.82	4.44	4.19	4.01	3.87	3.75	3.65	3.49
2.5	7.42	6.46	5.70	4.96	4.32	3.98	3.76	3.60	3.47	3.36	3.27	3.13
2	6.49	5.65	4.99	4.34	3.78	3.48	3.29	3.15	3.03	2.94	2.86	2.74
1.5	5.46	4.76	4.19	3.65	3.18	2.93	2.77	2.65	2.55	2.47	2.41	2.30
1	4.28	3.73	3.29	2.86	2.49	2.30	2.17	2.08	2.00	1.94	1.89	1.81
0.5	2.83	2.46	2.17	1.89	1.64	1.52	1.43	1.37	1.32	1.28	1.25	1.19
0	20	40	75	150	300	450	600	750	900	1050	1200	1500
	Power W											

Table 11 *Heat gain vs airflow for 2119 ft3*

ACHn	Predicted Neutral Height (ft) Volume-4238 ft³											
5	17.06	14.85	13.09	11.40	9.92	9.15	8.64	8.26	7.97	7.72	7.52	7.19
4.5	16.01	13.94	12.29	10.70	9.32	8.59	8.11	7.76	7.48	7.25	7.06	6.75
4	14.92	12.99	11.45	9.97	8.68	8.00	7.56	7.23	6.97	6.76	6.58	6.29
3.5	13.77	11.99	10.57	9.20	8.01	7.39	6.97	6.67	6.43	6.24	6.07	5.81
3	12.55	10.93	9.64	8.39	7.30	6.73	6.36	6.08	5.86	5.68	5.53	5.29
2.5	11.25	9.80	8.64	7.52	6.55	6.04	5.70	5.45	5.26	5.10	4.96	4.74
2	9.84	8.57	7.56	6.58	5.73	5.28	4.99	4.77	4.60	4.46	4.34	4.15
1.5	8.28	7.21	6.36	5.53	4.82	4.44	4.19	4.01	3.87	3.75	3.65	3.49
1	6.49	5.65	4.99	4.34	3.78	3.48	3.29	3.15	3.03	2.94	2.86	2.74
0.5	4.28	3.73	3.29	2.86	2.49	2.30	2.17	2.08	2.00	1.94	1.89	1.81
0	20	40	75	150	300	450	600	750	900	1050	1200	1500
	Power W											

It can be seen that when the heat gain in a space is at the larger end of this spectrum, and the airflow in a space is at the lower end, the model calculated neutral height is much lower than what was predicted early on in this research. As the size of the building increases, values that would be useful in the case of a DV system are seen in the outputs for the model calculated neutral heights. As previously stated, the values for the model calculated neutral height that coincide with the parameters that were used in this experiment cannot be validated using the experimental setup that was in place for the purposes of this research.

Table 10 shows the ratio of heat gain and airflow in a building with a similar volume to one of the buildings examined in the South Africa research by Ramsdell et al. (2015). The calculated neutral heights are similar to those calculated by the model for the test building that was used in this research. Further research into the actual conditions in a building of this size should be conducted in order to verify the conditions under which the building is thermally stratified.

CHAPTER 5: DISCUSSION AND CONCLUSION

The goal of this research was to simulate a building that was subject to high levels of infiltration and thermal stratification during the heating season, record the temperature distribution inside the building, and then use the data to validate a simplified method of modeling thermal stratification. After examining the data produced by this experiment in comparison with the model results, it was determined that further research in the area of developing a method for modeling buildings that are subject to high levels of infiltration in the heating season is needed before any firm conclusions can be drawn. It was initially predicted that the temperature profile in the test building would show thermal stratification with two different temperature gradients, and that a neutral height would develop in the upper portion of the space, marking the transition between the two gradients. The results show that the building is thermally stratified, however, the stratification may be closer to a linear temperature gradient, rather than having two different gradients as is found in DV systems. Further research in this area is needed to determine what types of temperature distributions occur in buildings with high levels of infiltration during the heating season.

The results produced by this experiment, specifically the modeling portion, suggest that if a neutral height does develop, that it is located lower in the space than what was predicted. Regardless of the location of the neutral height, the model only showed thermal stratification when the air-flow was set to a much higher rate than what was used in the experiment. As such, it would appear that the EnergyPlus™ Three-Node Displacement Ventilation RoomAir Model will not predict the temperature profiles in a test building that is subject to high levels of infiltration during the heating season within 10% accuracy. Furthermore, the results of this

research suggest that this modeling approach is most likely not the most appropriate method for modeling the building type in question. Here again, it is the opinion of the author that further research into the most appropriate method for modeling buildings subject to high levels of infiltration during the heating season is needed.

In terms of modeling the building types in the South Africa research being conducted by Ramsdell et al. (2015), and determining the levels of stratification and temperature distribution gradients present in these buildings, further research is needed. Even though high levels of air changes were simulated in the test building in this research, considering the tightness and insulation levels of the envelope of the building used in this experiment, further research should be performed before any conclusions can be made as to how much stratification is present in buildings that are constructed using simple techniques, with low levels of insulation and air sealing.

As was noted earlier in this paper, when there are large levels of heat transfer across a building's envelope, negatively buoyant convective currents at the ceiling and walls can develop with the same order of magnitude as those driving thermal plumes generated by heating appliances in a space, causing the airflow patterns in a zone to be more well mixed than one might assume (da Graça, 2003). When one considers the effectiveness of air sealing and insulation levels in the test building that was used in this research, it is conceivable that there is considerably less heat transfer across the envelope itself in the test building when compared with the heat transfer across the envelope of a building that contains little to no insulation and little to no air sealing. Because of this, it may be the case that the thermal stratification that was seen in the test structure was due solely to the induced air flow, and that the temperature distribution is atypical of what is seen in houses constructed using low levels of air sealing and insulation. For this reason, further research should be conducted in this area, so as to determine

the amount of error that is seen when applying energy modeling methods that assume that the air in the space is well mixed.

Following are some recommendations regarding setup of future research experiments in the area of modeling buildings that are subject to high levels of infiltration with low levels of insulation and air sealing, based on the findings from this research.

Sensor strands should be hung at even increments throughout the entire space. In this way a more accurate depiction of the space can be captured in the data collection. In the setup of the sensors in this research, the highest resolution strands were hung in a place where it was expected that the data would show the most notable neutral height. Not only were the assumptions that guided this portion of the setup wrong, they ultimately limited the data collection and resolution of temperature profiles in the space.

Sensor strands should have consistent sensor placement from the bottom of the strand to the top of the strand, allowing for consistent resolution. Here again, this portion of the setup was driven by assumptions made based on the expected outcomes, assuming that a neutral height would develop in the upper portion of the space. As such, no sensors were placed anywhere vertically between 4" and 48" in the space. This limited the ability of the author to make any firm conclusions on what the temperature profile looks like in this area.

Further research should be done using a test building constructed with simple techniques, in which zone conditions are representative of the heat and air transfer seen in the housing types that are examined in the South Africa research being conducted by Ramsdell et al. (2015). This is the most important part of the future research. In this way the amount of thermal stratification taking place in buildings of this type can be verified or denied. It is possible that buildings of this type are closer to well mixed than thermally stratified than one might assume, when one considers the amount of heat transfer that occurs across the envelope, and the resultant convective currents that are generated as a result.

More typical electrical gains should be used in the experiment, representative of heat gains from a person, as well as typical household electrical items (televisions, cooking appliances, etc.). As was seen in the literature review in this paper, even the smallest of heat gains can generate a thermal plume that might affect the air flow in a space. With all of the heat gains that are present in a typical home, this might lead to a more well mixed space than one might assume.

If meaningful recommendations are to be made regarding energy use in low income communities and developing nations as to the type of construction techniques and materials that should be used, a method for accurately modeling the interior conditions and energy use of these residences that is not overly computationally expensive should be developed. When such a large portion of population growth and urban development is occurring in areas of low income and energy insecurity, more and more people will be living in substandard conditions, and using energy sources that lead to pollution, low indoor environmental quality, and low occupant health. It is the responsibility of leaders in the building industry and the academic realm to strive to find a way for everyone to live in conditions deemed acceptable from the standpoint of health and comfort by the majority of the world's population. If humanity can move forward in the area of urban development with an eye towards energy efficiency, occupant comfort, and equal rights regarding basic human necessities such as housing, then we might be able to avoid some of the negative effects of unsustainable growth and in turn mitigate the worsening of climate instability that has resulted thus far.

REFERENCES

ASHRAE. (2019). *ASHRAE handbook*. Retrieved from https://handbook.ashrae.org/Handbook.aspx

Boyes, T. (2017). *An experimental case study of exterior water resistive barriers for stucco in Boone, North Carolina*. (Unpublished manuscript.) Appalachian State University, Boone, NC.

da Graça, G. C. (2003). *Simplified models for heat transfer in rooms* (Doctoral Dissertation). Retrieved from Academia.edu.

Daioglou, V., Van Ruijven, B.J, & Van Vuuren, D.P. (2012). Model projections for household energy use in developing countries. *Energy, 37,* 601-615.

Fan Affinity Laws. (2003). Retrieved from https://www.engineeringtoolbox.com/fan-affinity-laws-d_196.html

Griffith, B., & Chen, Y. (2004). Framework for coupling room air models to heat balance model load and energy calculations (RP-1222). *International Journal of Heating Ventilation Air Conditioning and Refrigerating Research*, (2), 91. Retrieved from http://search.ebscohost.com.proxy006.nclive.org/login.aspx?direct=true&db=edsbl&AN=RN166253146&site=eds-live&scope=site

Linden, P. F. (1999). The fluid mechanics of natural ventilation. *Annual Review of Fluid Mechanics, 31*, 201-238.

Linden, P.F., Lane-Serff, G.F. & Smeed, D.A. (1990). Emptying filling boxes: the fluid mechanics of natural ventilation. *Journal of Fluid Mechanics*, 212, 300-335.

Linden, P.F. and P. Cooper. (1996). Multiple sources of buoyancy in a naturally ventilated enclosure. *Journal of Fluid Mechanics*, 311, 177-192. https://doi.org/10.1017/S0022112096002558

ManualsLib. (2006). Retrieved from https://www.manualslib.com/manual/388934/Honeywell-Hz-2030-Safety-Sensor-Heater.html

ManualsLib. (2004). Retrieved from https://www.manualslib.com/manual/37192/Delonghi-2507l.html#manual

Mateus, N. M., & da Graça, C. G. (2015). A validated three-node model for displacement ventilation. *Building and Environment*, *84*, 50–59. Retrieved from https://doi-org.proxy006.nclive.org/10.1016/j.buildenv.2014.10.029

Morton, B. R., Taylor, G., & Turner, J. S. (1956). Turbulent gravitational convection from maintained and instantaneous sources. *Proceedings of the Royal Society of London. Series A, Mathematical and Physical Sciences*, *234*(1196), 1-23. Retrieved from http://search.ebscohost.com.proxy006.nclive.org/login.aspx?direct=true&db=edsjsr&AN=edsjsr.99936&site=eds-live&scope=site

Mulliner, E., Smallbone, K. & Maliene, V. (2013). An assessment of sustainable housing affordability using a multiple criteria decision making method. *Omega, 41,* 270-279.

Mundt, E. (1996). *The performance of displacement ventilation systems: Experimental and theoretical studies*. Ph. D. Thesis, Bulletin N38, Building Services Engineering KTH, Stockholm.

Population Reference Bureau. (2018). *2018 World population data* [Data sheet]. Retrieved from http://www.worldpopdata.org/

Ramsdell, J.E., Burkett, L.W., Davis, C.R., Delarm Neri, R., Jacobs, E., and Verster, J.J.P. (2015). Value of energy efficiency improvements for low-income housing in developing countries, presented at the 6th International Building Physics Conference (IBPC 2015). *Energy Procedia, 78,* 1021-1026.

Ramsdell, J.E., Delarm Neri, R., Jacobs, E., & Verster, J.J.P. (2012). *Energy efficiency improvements in residential South African structures using modern energy modelling techniques*. Paper presented at the International Cost Engineering Council World Congress (ICEC), Durban, South Africa, 2012. Sydney, Australia: ICEC Secretariat.

Rees, S.J. & Haves, P. 2001. A nodal model for displacement ventilation and chilled ceiling systems in office spaces. *Building and Environment, 36*(6), 753-762.

Walker, R. J. (2016). Population growth and its implications for global security. *American Journal of Economics and Sociology, 75*(4), 980-1004. doi: 10.1111/ajes.12161

U.S. Department of Energy. (2018a). *Engineering reference* (EnergyPlus™ Version 9.2.0 Documentation). Retrieved from https://bigladdersoftware.com/epx/docs/

U.S. Department of Energy. (2018b). Room air models. In *Input output reference* (EnergyPlus™ Documentation Version 9.2.0). Retrieved from https://bigladdersoftware.com/epx/docs/

Vita

Philip Howard was born on March 19, 1986, in Boone, North Carolina to Jack and Frances Howard. He attended public school in Avery county and graduated from Avery County High School in 2004. After high school, Mr. Howard attended Appalachian State University for a brief period of time before taking a break and returning to work for his father's propane distribution company. In 2015, Mr. Howard re-enrolled at Appalachian State to complete his undergraduate education in order to pursue a career in sustainability and energy efficiency in the built environment. Mr. Howard completed his Bachelor of Science degree in Building Science in 2017 and continued at Appalachian State in pursuit of a Master of Science degree. In December 2019, he completed the MS degree with a dual concentration in Sustainable Building Design and Construction and Appropriate Technology in the Department of Sustainable Technology and the Built Environment.